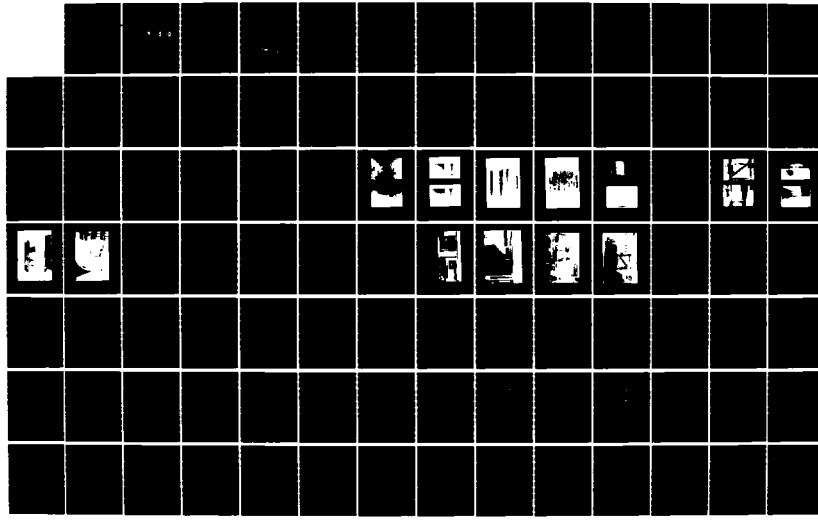


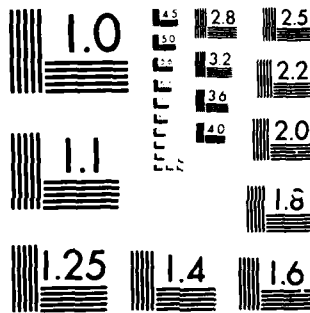
AD-A164 142 EXPERIMENTAL INVESTIGATION OF TURBULENT HEAT TRANSFER 1/2
IN STRAIGHT AND CURVED RECTANGULAR DUCTS(U) NAVAL
POSTGRADUATE SCHOOL MONTEREY CA G G GALVO DEC 85

UNCLASSIFIED

F/G 20/13

NL





MICROCOPY RESOLUTION TEST CHART
© 1984 by E.A. MULLEN & CO., INC.

AD-A164 142

NAVAL POSTGRADUATE SCHOOL
Monterey, California



DTIC
ELECTED
FEB 14 1986
S A D

THESIS

EXPERIMENTAL INVESTIGATION OF TURBULENT HEAT
TRANSFER IN STRAIGHT AND CURVED
RECTANGULAR DUCTS

by

George Gregory Galyo

December 1985

Thesis Advisor:

M. D. Kelleher

Approved for public release; distribution is unlimited

DTIC FILE COPY

86 2 14 044

AD A164 11

REPORT DOCUMENTATION PAGE

1a REPORT SECURITY CLASSIFICATION UNCLASSIFIED		1b. RESTRICTIVE MARKINGS	
2a SECURITY CLASSIFICATION AUTHORITY		3 DISTRIBUTION/AVAILABILITY OF REPORT Approved for public release; distribution is unlimited	
2b DECLASSIFICATION/DOWNGRADING SCHEDULE			
4 PERFORMING ORGANIZATION REPORT NUMBER(S)		5 MONITORING ORGANIZATION REPORT NUMBER(S)	
6a NAME OF PERFORMING ORGANIZATION Naval Postgraduate School	6b OFFICE SYMBOL (If applicable) 69	7a. NAME OF MONITORING ORGANIZATION Naval Postgraduate School	
6c. ADDRESS (City, State, and ZIP Code) Monterey, California 93943-5100		7b. ADDRESS (City, State, and ZIP Code) Monterey, California 93943-5100	
8a NAME OF FUNDING / SPONSORING ORGANIZATION	8b. OFFICE SYMBOL (If applicable)	9. PROCUREMENT INSTRUMENT IDENTIFICATION NUMBER	
8c ADDRESS (City, State, and ZIP Code)		10 SOURCE OF FUNDING NUMBERS	
		PROGRAM ELEMENT NO	PROJECT NO
		TASK NO	WORK UNIT ACCESSION NO
11 TITLE (Include Security Classification) EXPERIMENTAL INVESTIGATION OF TURBULENT HEAT TRANSFER IN STRAIGHT AND CURVED RECTANGULAR DUCTS			
12 PERSONAL AUTHOR(S) George Gregory Galyo			
13a TYPE OF REPORT Master's Thesis	13b TIME COVERED FROM _____ TO _____	14 DATE OF REPORT (Year, Month, Day) 1985 December	15 PAGE COUNT 110
16 SUPPLEMENTARY NOTATION			
17 COSATI CODES		18 SUBJECT TERMS (Continue on reverse if necessary and identify by block number) Taylor-Gortler Vortices, Dean Number, Heat Transfer, Turbulent Flow, Rectangular Curved Channel, Rectangular Straight Channel, Secondary Flow, Concave, Convex	
19 ABSTRACT (Continue on reverse if necessary and identify by block number) An experimental apparatus has been constructed and tested to examine the convective heat transfer in straight and curved ducts of rectangular cross-section. The channel can be configured with both walls independently heated at a constant heat flux, or one wall at a constant heat flux and the opposite wall adiabatic. Local and average Nusselt numbers can be calculated, and used to evaluate the effect of curvature on heat transfer.			
Experiments were conducted at steady state for turbulent flow with one wall heated at a constant flux and the opposite wall adiabatic. The heat transfer characteristics of the straight and curved sections, on both the inner and outer walls, were compared. The heat transfer rate of the concave curved wall proved to be enhanced over both the convex curved wall and both straight sections. THESE RESULTS ARE NOT FOR REFLECTION			
20 DISTRIBUTION/AVAILABILITY OF ABSTRACT <input checked="" type="checkbox"/> UNCLASSIFIED/UNLIMITED <input type="checkbox"/> SAME AS RPT. <input type="checkbox"/> DTIC USERS		21. ABSTRACT SECURITY CLASSIFICATION UNCLASSIFIED	
22a NAME OF RESPONSIBLE INDIVIDUAL Matthew D. Kelleher		22b TELEPHONE (Include Area Code) (408) 646-2530	22c. OFFICE SYMBOL 69Kk

Approved for public release; distribution is unlimited

Experimental Investigation of Turbulent Heat Transfer
in Straight and Curved Rectangular Ducts

by

George Gregory Galyo
Lieutenant, United States Navy
B.S., United States Naval Academy, 1980

Submitted in partial fulfillment of the
requirements for the degree of

MASTER OF SCIENCE IN MECHANICAL ENGINEERING

from the

NAVAL POSTGRADUATE SCHOOL
December 1985

Author:

George Gregory Galyo
George Gregory Galyo

Approved by:

Matthew D. Kelleher
Matthew D. Kelleher, Thesis Advisor

P.J. Mardo
Paul J. Mardo, Chairman, Department of
Mechanical Engineering

J.N. Dyer
J. N. Dyer, Dean of Science and Engineering

ABSTRACT

An experimental apparatus has been constructed and tested to examine the convective heat transfer in straight and curved ducts of rectangular cross-section. The channel can be configured with both walls independently heated at a constant heat flux, or one wall at a constant heat flux and the opposite wall adiabatic. Local and average Nusselt numbers can be calculated, and used to evaluate the effect of curvature on heat transfer.

Experiments were conducted at steady state for turbulent flow with one wall heated at a constant heat flux and the opposite wall adiabatic. The heat transfer characteristics of the straight and curved sections, on both the inner and outer walls, were compared. The heat transfer rate of the concave curved wall proved to be enhanced over both the convex curved wall and both straight sections.

Accession For	
NTIS CRA&I <input checked="" type="checkbox"/>	
DTIC TAB <input type="checkbox"/>	
Unannounced <input type="checkbox"/>	
Justification	
By	
Distribution /	
Availability Codes	
Dist	Avail and/or Special
A-1	

TABLE OF CONTENTS

I.	INTRODUCTION	13
A.	TAYLOR-GORTLER VORTICES	13
B.	HISTORY	15
II.	INTENT OF STUDY	22
III.	EXPERIMENTAL SETUP	25
A.	DESCRIPTION OF THE APPARATUS	25
B.	DETAILS OF THE CONSTRUCTION	29
C.	INSTRUMENTATION	43
IV.	EXPERIMENTAL PROCEDURES	51
V.	PRESNTATION OF DATA	55
A.	DATA REDUCTION	55
B.	RESULTS	57
VI.	DISCUSSION AND CONCLUSIONS	69
VII.	RECOMMENDATIONS	79
APPENDIX A:	COMPUTER PROGRAM	81
APPENDIX B:	SAMPLE CALCULATIONS	91
1.	SAMPLE CALCULATION DATA	92
2.	TEMPERATURE CALCULATIONS	95
3.	POWER CALCULATIONS	96
4.	MASS FLOW RATE CALCULATIONS	97
5.	REYNOLDS NUMBER CALCULATIONS	99
6.	HEAT CONVECTED TO AIR CALCULATION	99

7. AVERAGE HEAT TRANSFER COEFFICIENT CALCULATION	99
8. AVERAGE NUSSELT NUMBER CALCULATION	99
9. DEAN NUMBER CALCULATION	100
APPENDIX C: EXPERIMENTAL UNCERTAINTY	101
LIST OF REFERENCES	106
INITIAL DISTRIBUTION LIST	109

LIST OF TABLES

I.	SUMMARY OF STRAIGHT OUTER WALL TEST RESULTS	58
II.	SUMMARY OF STRAIGHT INNER WALL TEST RESULTS	59
III.	SUMMARY OF CURVED CONCAVE WALL TEST RESULTS	60
IV.	SUMMARY OF CURVED CONVEX WALL TEST RESULTS	61

LIST OF FIGURES

1.	Schematic of Taylor-Gortler Vortices in a Curved Channel	14
2.	Schematic of Taylor Vortices between Cylinders . . .	17
3.	Schematic Cross-sectional View of Channel	26
4.	Schematic of Rectangular Channel	27
5.	Thermocouple Placement in Copper Plates	30
6.	Photograph of Milled Thermocouple Slots	32
7.	Photograph of Thermocouple Placement Holes	32
8.	Photograph of Both Inner Plates Showing Slot Pattern	33
9.	Photograph of Both Outer Plates Showing Slot Pattern	33
10.	Photograph of Epoxied Thermocouples in Outer Curved Plate	34
11.	Photograph of Epoxied Thermocouples in Outer Straight Plate	35
12.	Photograph of Convex Surface of Copper Plate	36
13.	Photograph of Completed Heated Test Section	36
14.	Photograph of Channel Frame	38
15.	Photograph of Bottom View of Inner Straight Test Section	38
16.	Photograph of Inner Straight Wall at Copper-Plexiglas Joint	39
17.	Photograph of Inner Curved Wall at Copper-Plexiglas Joint	39
18.	Photograph of Outer Frame and Lexan Wall Showing Straight Test Section	40

19.	Photograph of Outer Curved Test Section	41
20.	Power Measurement Circuit	45
21.	Photograph of Data Acquisition System	47
22.	Photograph of Flow Measuring Apparatus	48
23.	Photograph of Spencer Turbo Compressor	49
24.	Photograph of Test Channel	50
25.	Present Straight vs. Curved Section Results	62
26.	Present Concave vs. Convex Section Results	63
27.	Present Straight Outer vs. Inner Section Results	64
28.	Present Concave vs. Straight Outer Section Results	65
29.	Present Convex vs. Straight Inner Section Results	66
30.	Comparison of Present Data with Daughety and Wilson, Curved Section	71
31.	Comparison of Present Data with Daughety and Wilson, Straight Section	72
32.	Comparison of Present Data with Daughety and Corrected Wilson, Curved Section	73
33.	Comparison of Present Data with Daughety and Corrected Wilson, Straight Section	74
34.	Comparison of Present Data with Dittus-Boelter, Kays and Leung, for Turbulent Flow, Straight Section	76
35.	Comparison of Present Data with Brinich and Graham, and Kreith, for Turbulent Flows, Curved Section	78
36.	Energy Balance in Test Section	91

LIST OF SYMBOLS

<u>Symbol</u>	<u>Meaning</u>	<u>Units</u>
A	cross-sectional area of the orifice	m^2
A_c	cross-sectional area of the channel	m^2
A_{pipe}	cross-sectional area of the pipe	m^2
A_{PL}	area of the heated wall	m^2
C_{pair}	specific heat of air at constant pressure	J/KgK
D _c	channel height	m
D _e	Dean number	
D _{hd}	hydraulic diameter	m
D _{orf}	diameter of the orifice	m
D _{pipe}	diameter of the pipe	m
F _{wo-wi}	radiation shape factor	
g_c		$\frac{\text{Kg m}}{\text{N sec}}^2$
\bar{h}	average heat transfer coefficient	$\text{W/m}^2\text{C}$
K	flow coefficient	
K _{air}	thermal conductivity of air	W/mC
K _{ins}	thermal conductivity of insulation	W/mC
\dot{m}	mass flow rate of air	Kg/sec
Nu	local Nusselt number	
$\overline{\text{Nu}}$	average Nusselt number	
Pr	Prandtl number	
P _{atm}	atmospheric pressure	N/m^2

<u>Symbol</u>	<u>Meaning</u>	<u>Units</u>
P_1	pressure upstream of orifice	N/m ²
P_{wet}	wetted perimeter of channel	m
Q_{air}	heat convected to air	W
Q_{li}	heat lost through inner wall	W
Q_{lo}	heat lost through outer wall	W
Q_p	power supplied	W
Q_r	heat transferred by radiation	W
R	gas constant for air	Nm/Kg K
Re_d	Reynolds number based on channel height	
Re_{hd}	Reynolds number based on hydraulic diameter	
Re_{pipe}	Reynolds number based on pipe diameter	
R_i	radius of curvature of inner convex wall	m
R_{PR}	electrical resistance of precision resistor	Ω
R_R	total radiation resistance	m^{-2}
Ta	Taylor number	
T_{blk}	bulk temperature of flow	C
T_{in}	average flow inlet temperature	C
$T_{ins,i1}$	temperature between Plexiglas and first layer of inner insulation	C
$T_{ins,i2}$	temperature between first and second layers of inner insulation	C
$T_{ins,i3}$	temperature between second and third layers of inner insulation	C
$T_{ins,o1}$	temperature between Lexan and first layer of outer insulation	C
$T_{ins,o2}$	temperature between first and second layers of outer insulation	C

<u>Symbol</u>	<u>Meaning</u>	<u>Units</u>
$T_{ins,o3}$	temperature between second and third layers of outer insulation	C
T_{orf}	temperature of air flowing downstream of orifice	C
T_{out}	average flow outlet temperature	C
T_{wi}	average temperature of inner wall	C
T_{wo}	average temperature of outer wall	C
V_{PR}	voltage across precision resistor	V
V_H	voltage across the wall heater	V
W_{id}	width of channel	m
γ	expansion factor	
β	ratio of orifice diameter to pipe diameter	
ϵ_{cu}	emissivity of copper plate	
γ	ratio of specific heats of air	
μ_{air}	dynamic viscosity of air	Kg/m sec
ρ_{air}	density of air	Kg/m ³
σ	Stefan-Boltzmann constant	W/m ² K ⁴
ΔP	pressure drop across the orifice	N/m ²
ΔT	mean temperature difference	C
Δx_{ins}	thickness of insulation layer	m

ACKNOWLEDGEMENT

The author wishes to express his deep appreciation to Professor Matthew D. Kelleher for his insight and guidance throughout all phases of this project. His experience and assistance made the work on this thesis a valuable learning experience. Also, a special thanks to Dr. Amarawansa Wanniarachchi for his assistance in developing and writing the computer program used to gather and reduce the data. In addition, Mr. Charles Crow deserves a special thanks for all his work and effort in the construction of the experimental channel.

Finally, the author wishes to thanks his wife Susan and daughter Michelle for all their sacrifices and encouragement during this course of study.

I. INTRODUCTION

A. TAYLOR-GORTLER VORTICES

Since the early part of the twentieth century, considerable research has shown that the fully developed laminar flow along a concave wall does not remain two-dimensional [Refs. 1, 2, 3]. The flow instead forms a system of spiral vortices, of counter rotating pairs, whose axes are aligned in the principle flow direction. This phenomenon is the result of the variations in the centrifugal forces acting on the fluid particles, and is known as Taylor-Gortler vortices. Figure 1 illustrates the type of fluid motion just described.

In a channel that is curved in the streamwise direction, those fluid particles located in the center of the flow cross-section are subject to higher centrifugal forces than those fluid particles traveling along the channel's outer boundary wall. As a result, the fluid in the center of the channel moves outwardly toward the concave boundary. As the process continues, the fluid particles near the boundary wall, move in a spanwise direction, and finally radially inward replacing the outwardly moving particles. These particles then come under the same centrifugal force and the process repeats itself. The resulting cyclic motion causes the formation of the counter rotating Taylor-Gortler

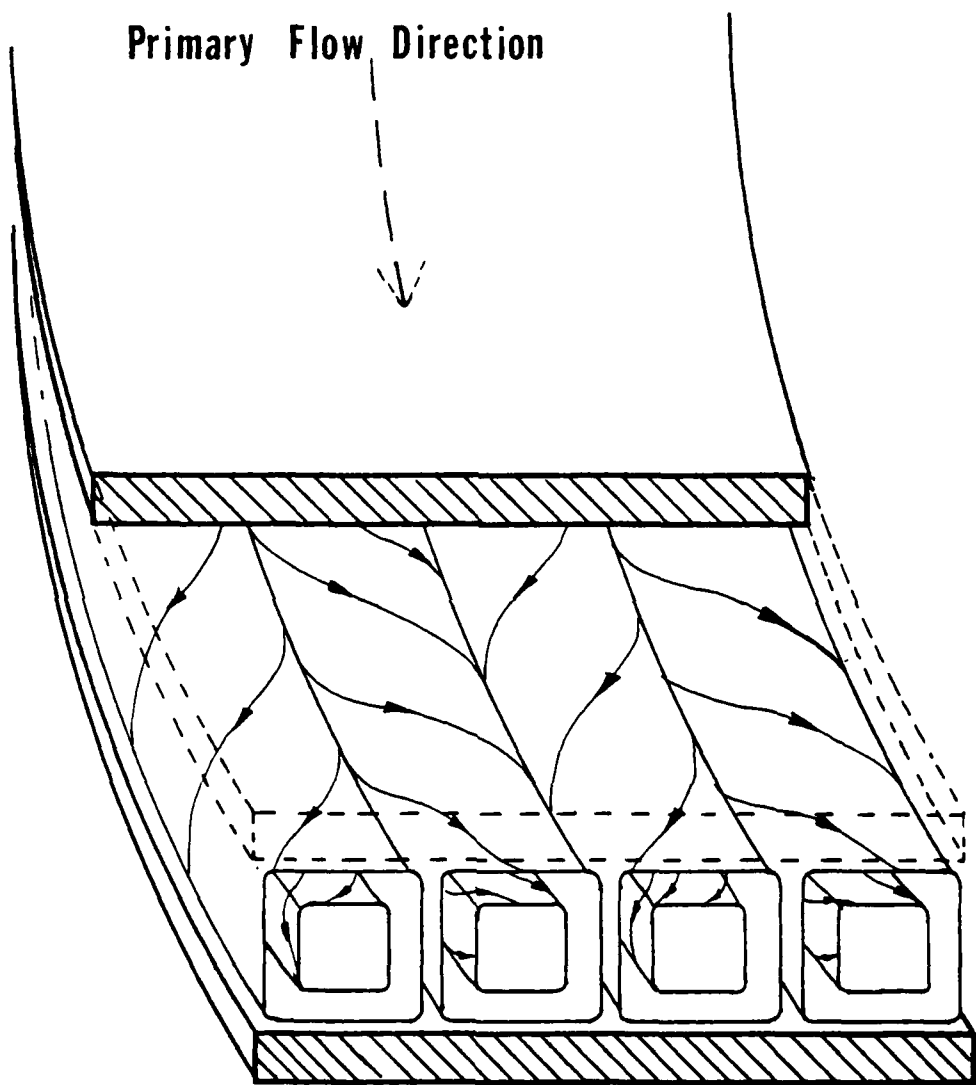


Figure 1. Schematic of Taylor-Görtler Vortices in a Curved Channel.

vortices, considered to be primarily a laminar flow phenomenon.

It has been observed [Ref. 4] that the heat transfer rate from flow along a concave curved wall is greater than that for flow along a straight wall, a phenomenon attributed to the additional mixing provided by the secondary motion of the Taylor-Gortler vortices.

There are many possible applications that could result from a more thorough understanding of Taylor-Gortler vortices and their effect on heat transfer and fluid flow characteristics. Two such applications could lead to improved heat exchanger designs and improved turbine blade cooling [Refs. 5, 6, 7].

B. HISTORY

The stability of an inviscid fluid flowing past a curved boundary, was first considered by Lord Rayleigh in 1916 [Ref. 8]. By assuming that the fluid was non-viscous, he determined that for the motion to remain stable, its circulation must increase with increasing radius. G. I. Taylor, in 1923, [Refs. 1, 9], continued this study with an extensive analytical and experimental study of viscous fluids. His investigations focused on the flow between two cylinders, in which the inner cylinder rotated while the outer cylinder remained stationary. Taylor ascertained that such flows become unstable when the value of a dimensionless parameter exceeded a critical value of 41.3.

The parameter, known as the Taylor number is defined as:

$$Ta = Re \sqrt{d/Ri}$$

where 'd' is the width of the gap, assumed small when compared to 'Ri', the radius of the inner cylinder, and 'Re' is the Reynolds number based on the peripheral velocity of the inner cylinder. Taylor determined that for those cases in which the value of the Taylor number exceeded the critical value, a secondary motion developed and the Taylor vortices formed. Figure 2 illustrates this fluid motion.

Instability of a similar nature is also observed when a viscous fluid flows in a curved channel due to a pressure gradient acting along the channel wall. This problem was first considered analytically by W. R. Dean [Ref. 10] in 1928, for a channel formed by two concentric cylinders, where the radius of the inner cylinder was large in comparison to the spacing between the inner and outer cylinder walls. Dean concluded that there would be an initiation of flow instability, and the formation of vortices, when a dimensionless parameter, the Dean number, exceeded a value of 36. The Dean number is defined as:

$$De = Re \sqrt{\frac{d}{Ri}}$$

where 'd' represents the channel half-width, 'Ri' is the inner cylinder radius, and 'Re' is the Reynolds number based

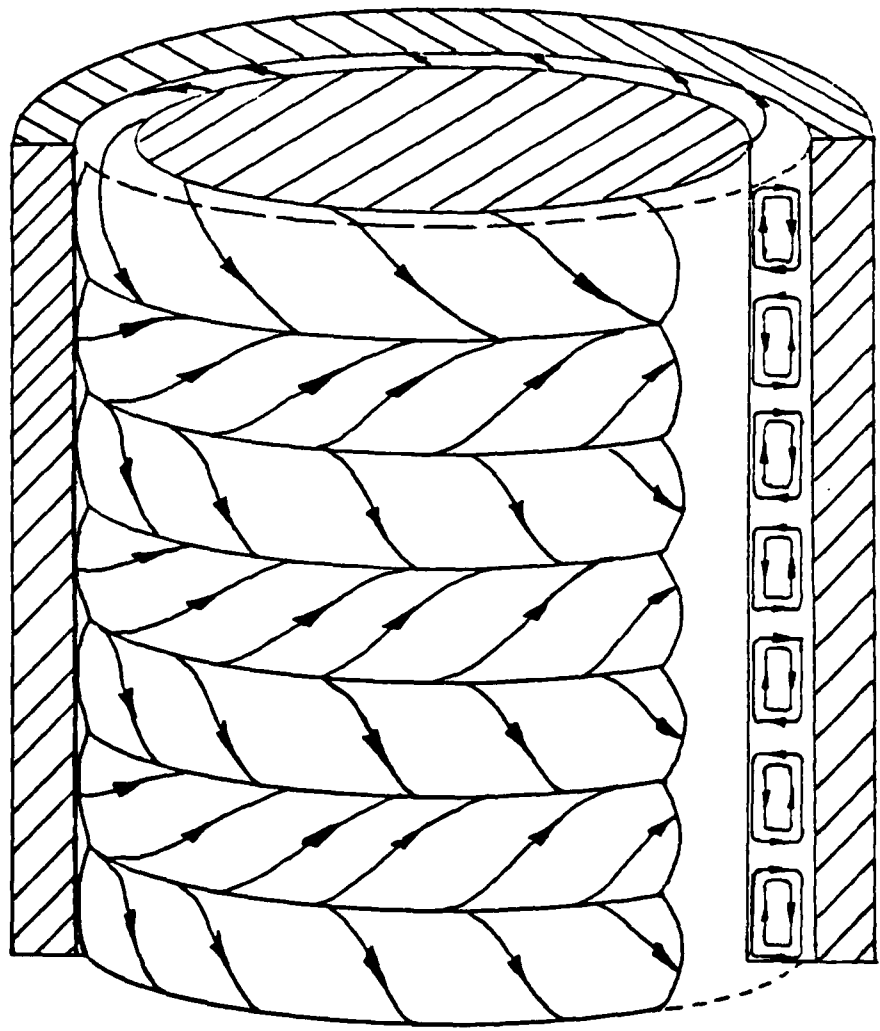


Figure 2. Schematic of Taylor Vortices between Cylinders.

on the mean velocity of the undisturbed flow and the channel half-width 'd'. The analytical work of Dean was later verified by W. H. Reid [Ref. 11], using an approximate solution.

In 1940, H. Gortler [Ref. 2] studied the stability of laminar boundary layer profiles on curved walls under the influence of small disturbances. He found that these disturbances were similar to the vortices studied by G. I. Taylor. Using approximate numerical calculations, Gortler concluded that the disturbances of vortices were produced only on the concave boundary walls and that the overall flow profile appeared to remain laminar in nature. These results were verified, with an exact solution, by G. Hammerlin, and reported by H. Schlichting [Ref. 12] in 1955. A. M. O. Smith completed an even more extensive numerical analysis that further substantiated these findings [Ref. 3]. The results of these numerical solutions have recently been demonstrated with the use of hot wire anemometry, laser doppler systems, and flow visualizations techniques, [Refs. 13, 14]; and in 1976, Y. Aihara [Ref. 15] conducted a non-linear analysis of Gortler Vortices.

As interest began to develop concerning the effects of the secondary flows associated with the Taylor-Gortler vortices, many studies were published concerning the influences of these vortices on heat transfer in the laminar

and turbulent flow regimes. In 1955, F. Kreith [Ref. 16], studied the influence of heat transfer with respect to the curvature of the boundary wall for fully turbulent flows. He concluded that the heat transfer from the heated concave boundary wall was considerably higher than that transferred from the convex boundary wall of the same curvature and under similar turbulent conditions.

In 1965, L. Persen [Ref. 17], considered the special cases of very high and very low Prandtl number fluids and related the increase in heat transfer from a curved wall to the presence of the Taylor-Gortler vortices.

There has been only a limited amount of published literature dealing with the flow and heat transfer in curved channels of rectangular cross-section and large aspect ratios, where the aspect ratio is equal to the spanwise distance of the channel divided by the channel height. Much of what has been published involves the development of numerical approximations and solutions for heat and mass transfer in curved ducts of various geometries. K. Cheng and M. Akiyama [Ref. 18] developed a numerical solution for forced convection heat transfer with laminar flows in curved channels of rectangular cross-section, but only for small aspect ratios.

In 1976, A. A. Shirani and M. N. Ozisik [Ref. 19], using matched asymptotic expansion techniques for a wide range of

Prandtl numbers, solved the heat transfer problem between straight parallel plates with turbulent flow, for the case of uniform wall temperature.

Other experimental and analytical studies that are worth citing with regard to this present study are Y. Mori [Ref. 20], who obtained results for hydrodynamically fully developed flows with constant wall heat flux in curved channels of square cross-section. W. M. Kays and E. Y. Leung [Ref. 21] reported solutions for turbulent flow heat transfer in a concentric circular tube annulus with a fully developed velocity profile and constant heat rate per unit length, for a fluid of Prandtl number 0.7. P. F. Brinich and R. W. Graham [Ref. 22] reported results for turbulent flows in a rectangular curved channel with an aspect ratio of 6, for the inner wall heated, the outer wall heated, and both walls heated.

In 1973, at the Naval Postgraduate School, R. J. McKee [Ref. 23] confirmed the presence of Taylor-Gortler vortices in a curved rectangular channel of aspect ratio 40. M. Durao [Ref. 24] modified R. J. McKee's channel and modeled it as infinite parallel plates with the outer wall heated and inner wall adiabatic. M. Durao and J. Ballard [Refs. 24, 25] investigated the effects of Taylor-Gortler vortices on the heat transfer in a straight and curved test section for laminar flows. R. Holihan, Jr. [Ref. 26] reported

results for laminar and transition flows. S. Daughety [Ref. 27] reported results for turbulent flows and J. Wilson [Ref. 28] reported results for transition and turbulent flows. Each time McKee's apparatus was used it was modified slightly using prior recommendations to improve on the accuracy of the results.

II. INTENT OF STUDY

The purpose of this investigation was to build an improved curved rectangular duct of large aspect ratio which could be configured with a variety of boundary conditions, and yield more accurate data than previously attained. By combining new ideas and experimental equipment with past experiences and recommendations of R. McKee and others previously mentioned [Refs. 23, 24, 25, 26, 27, 28], the effect of streamwise curvature on the heat transfer rate in a curved rectangular channel could be studied in greater detail while providing a smaller uncertainty in the results.

Some of the improvements incorporated in the new channel include: the ability to heat one or both walls over a wide range of constant heat fluxes; the ability to heat both walls at different constant heat fluxes; the use of more calibrated thermocouples which will allow greater precision in reading surface and air stream temperatures, combined with a better arrangement which will allow the calculation of the local heat transfer coefficient and Nusselt number; a longer transition region at the outlet which will allow for more mixing and a more accurate outlet temperature measurement. The use of an outer and inner section allowed both wall surfaces to be specially constructed with smooth

transitions between wall and heater surfaces in both straight and curved test sections, preventing unexpected tripping from laminar to turbulent flow. Finally, by constructing the channel with materials having low thermal conductivities and avoiding any heat sinks along the channel walls, heat losses could be minimized.

Taylor-Gortler vortices are known to enhance heat transfer in curved channels for transition and turbulent flows. This enhancement in the transfer of heat has been attributed to the secondary flow velocity components of the Taylor-Gortler vortices. These secondary components transport the heated fluid from the outer concave wall, inward toward the opposite wall of the channel, displacing the cooler fluid particles and causing them to move toward the heated concave wall. It was expected that similar results would be observed in this study.

This investigation was conducted using a single channel with a rectangular cross-section and constant aspect ratio, again defining aspect ratio as the spanwise distance divided by the channel height. The channel incorporates a straight and a curved test section. Each test section consists of opposing walls which can be independently heated. The results obtained in each test section at approximately the same flow rates were compared in an effort to determine the effects of the Taylor-Gortler vortices on the heat transfer

rate. Also, the results of both the straight and curved outer sections were compared to the results of Daughety [Ref. 27], and Wilson [Ref. 28] to compare the new channel to the old one.

The straight section results of this study were compared to the Dittus-Boelter correlation using hydraulic diameter [Ref. 29], and the results of Kays and Leung for turbulent and transition flow in annular passages [Ref. 21].

The curved section results of this study were compared with the results of Brinich and Graham [Ref. 22] for turbulent flow in a rectangular curved channel, and with Kreith [Ref. 16] for turbulent flows in concave and convex curved channels.

III. EXPERIMENTAL SETUP

A. DESCRIPTION OF THE APPARATUS

To meet the objectives of this investigation, a channel of rectangular cross-section and constant aspect ratio was constructed. The rectangular channel has four electrically heated wall sections, composed of a rubber heater bonded to a thin copper plate. All four heated wall sections are 30.48 centimeters long and 25.4 centimeters wide, with a heated area of 774.2 square centimeters. The rectangular channel is 0.635 centimeters high and 25.4 centimeters wide resulting in an aspect ratio of 40. The cross-sectional area of the channel is 16.13 square centimeters. The wetted perimeter is 52.07 centimeters, and the hydraulic diameter is 1.239 centimeters. Figure 3 shows a cross-sectional view presenting both the straight and curved sections of the channel.

The channel, shown in Figure 4, has a straight entrance region of 76.20 centimeters, which insures hydrodynamically fully developed flow prior to entering the straight heated test sections. The entrance region is followed by two parallel 30.48 centimeter straight heated test sections, which oppose each other, one in each wall. Following the straight heated test sections is a 15.32 centimeter straight

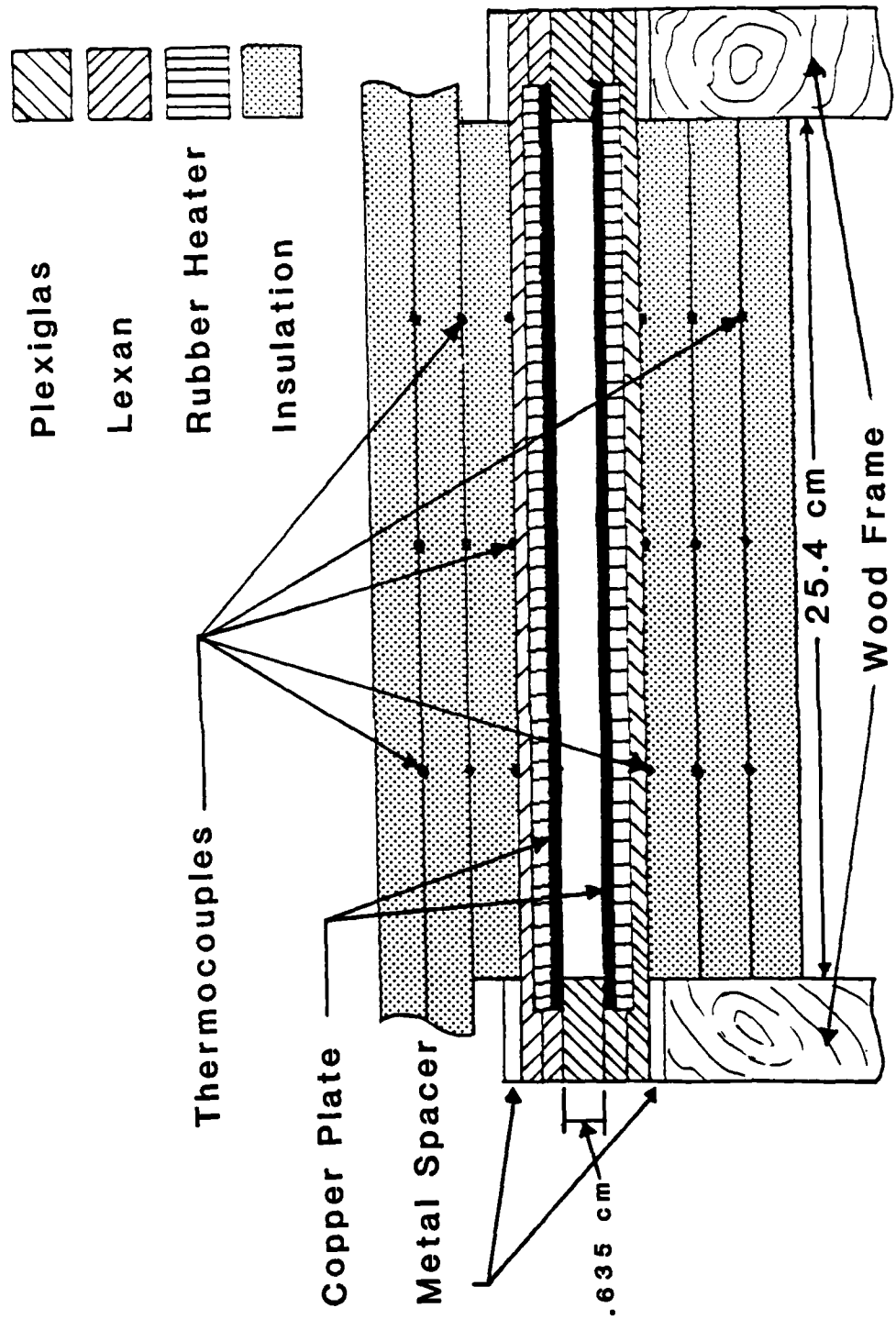


Figure 3. Schematic Cross-sectional View of Channel.

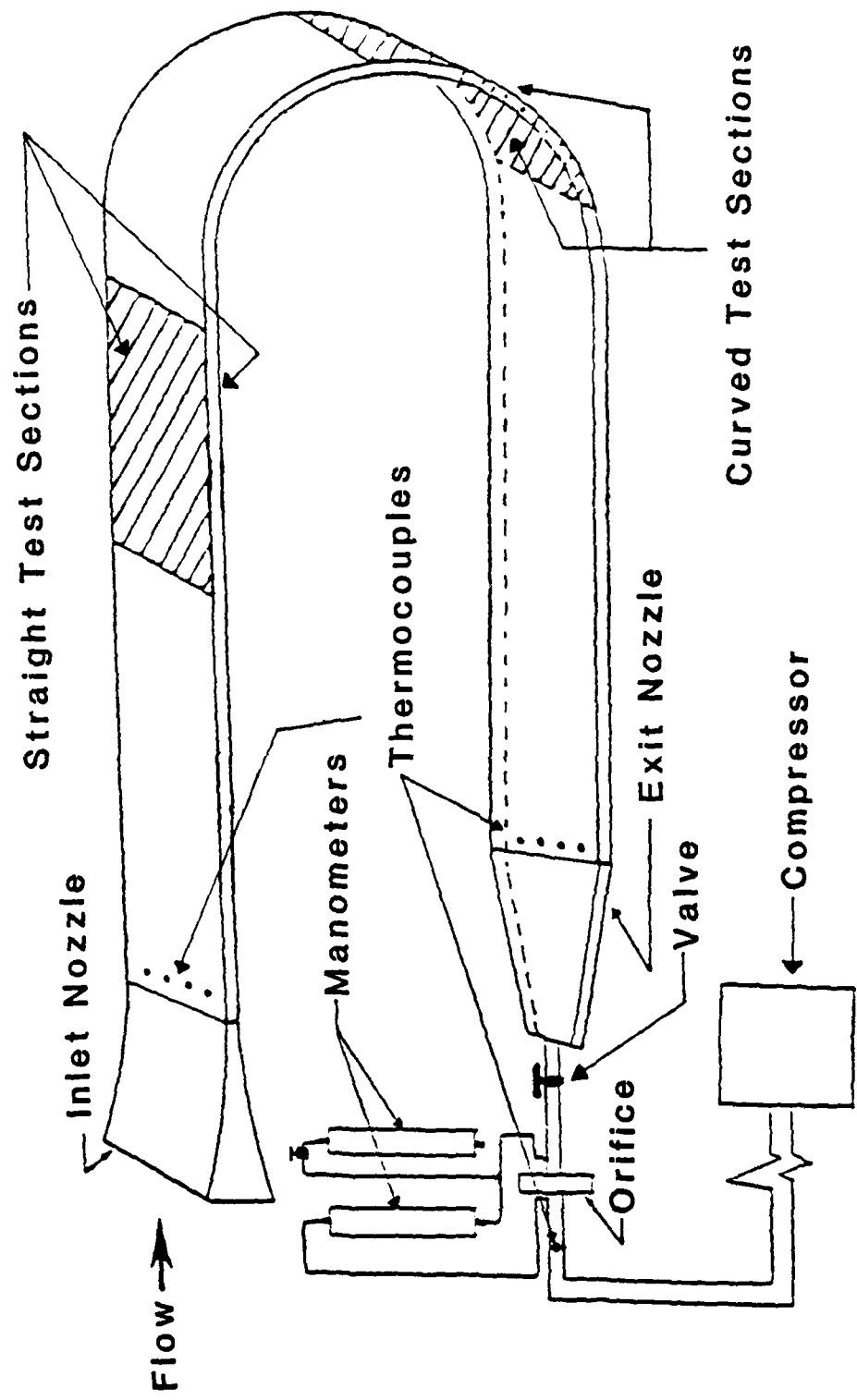


Figure 4. Schematic of Rectangular Channel.

exit region, that completes the straight test section. The straight test section is immediately followed by the curved test section which subtends a 180 degree arc, with the inner wall having a radius of curvature of 29.7 centimeters. The curved test section has a 52.63 centimeter unheated convex curved section prior to the curved heated sections. The two concentric curved heated sections, inner one convex and outer one concave, are 30.48 centimeters long and the outer heated wall subtends an arc of 58.8 degrees. The curved heated sections are followed by a 10.16 centimeter convex curved exit region which completes the curved test section. Finally, the channel is completed by a 92.0 centimeter straight exit region which allows sufficient mixing prior to reading the outlet temperature. The entire channel was then thermally insulated with a plastic foam material.

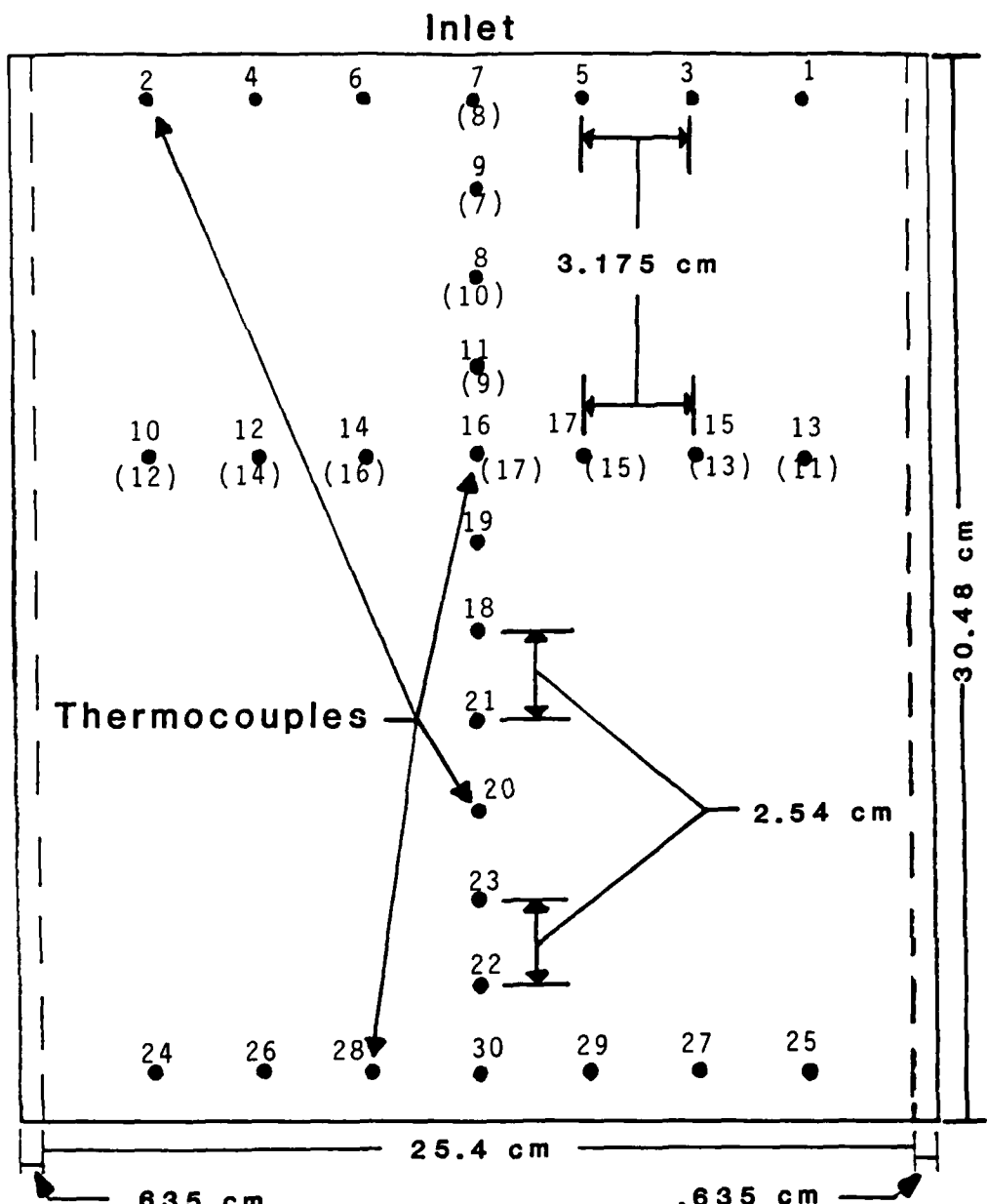
An entrance bell constructed of Plexiglas is connected to the inlet of the straight entrance section of the channel. It was designed and manufactured according to ASME nozzle standards, with an elliptical curved base on a major axis equal to 25.4 centimeters and a minor axis of 2.54 centimeters. A fiberglass filter was attached to the entrance nozzle to prevent foreign matter from entering the channel. An aluminum exhaust nozzle was attached to the exit of the channel and directed the flow from the channel into a two inch diameter pvc pipe. The piping contained a

mass flow rate measuring section which could be fitted with standard ASME concentric orifices.

A total of one hundred and eighty-nine copper-constantan, 30 gauge thermocouples are located throughout the test apparatus. Only ninety-nine thermocouples are read at anyone time, through seventy-five data channels, to record the desired temperatures. Each heated wall section contains thirty thermocouples which are read individually and then averaged to give the wall section surface temperature. Four thermocouples span the width of the channel at the entrance and exit to give the average entrance and exit air temperatures. Three groups of five thermocouples are connected in parallel and inserted between each layer of insulation at each of the heated test sections. Each group of five thermocouples only uses one data channel, and these extra thermocouples comprise the difference between the number of thermocouples read and the data channels available. Finally, there is one thermocouple to measure the air temperature at the orifice.

B. DETAILS OF THE CONSTRUCTION

Each of the four heated wall sections was composed of a copper plate laminated to a wire wound silicone rubber heater. The rubber heater was made by Watlow Industries. There are thirty copper-constantan thermocouples placed between the copper plate and rubber heater. Figure 5 shows



Outlet

Legend: numbers above location marks are outer and inner thermocouple numbers, numbers in parentheses below location mark apply to inner plates only.

Figure 5. Thermocouple Placement in Copper Plates.

the placement of the thermocouples on the back of the copper plate. The copper plate is 30.48 centimeters long, 26.72 centimeters wide, and 0.155 centimeters thick, but only the middle 25.4 centimeters of copper plate width is heated and centered in the channel. The back of the copper plate has a pattern of slots milled 0.076 centimeters deep. The pattern of slots for the two inner plates is different from the pattern of slots for the two outer plates. See Figures 6, 7, 8, and 9. The calibrated thermocouples were numbered and epoxied into the slots, as shown in Figures 10 and 11. The rubber heater has the same length and width dimensions as the copper plate, but only heats the middle 25.4 centimeters of width. This results in a heated wall area of 774.2 square centimeters. The excess copper plate is sandwiched between the wall and the side spacer thereby helping to support the copper plate in the channel. Dow Corning 3140 RTV was used to adhere the rubber heater to the back of the copper plate, and complete the heated section. Figure 12 and 13 represent a completed test wall.

The channel was built on a carefully constructed wood frame with steel rails, that also was used to support the entire channel. The inner wall was composed of two 0.343 centimeter thick and 29.85 centimeter wide pieces of Plexiglas laminated together, that had spaces milled out for the heated copper sections. The inner wall was constructed

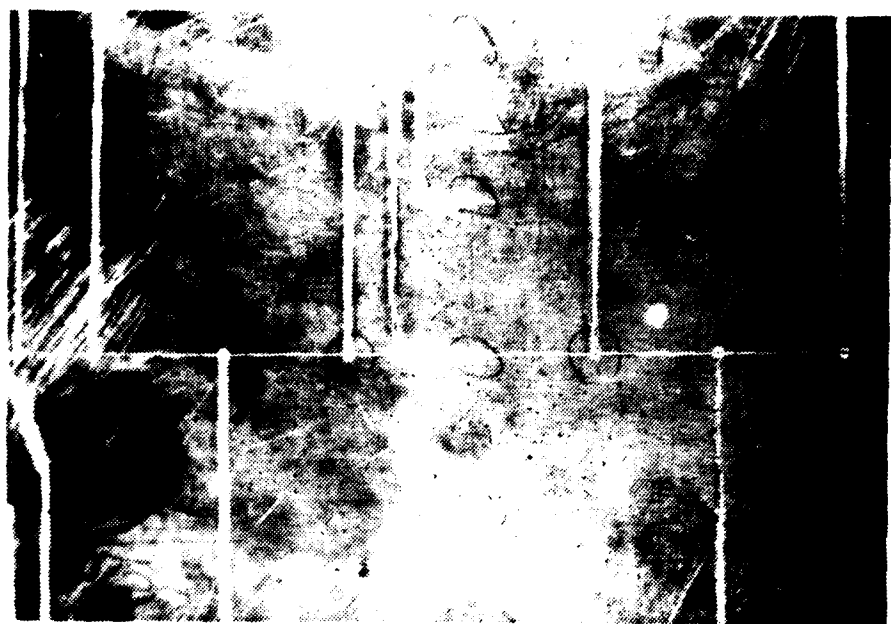


Figure 6. Photograph of Milled Thermocouple Slots.

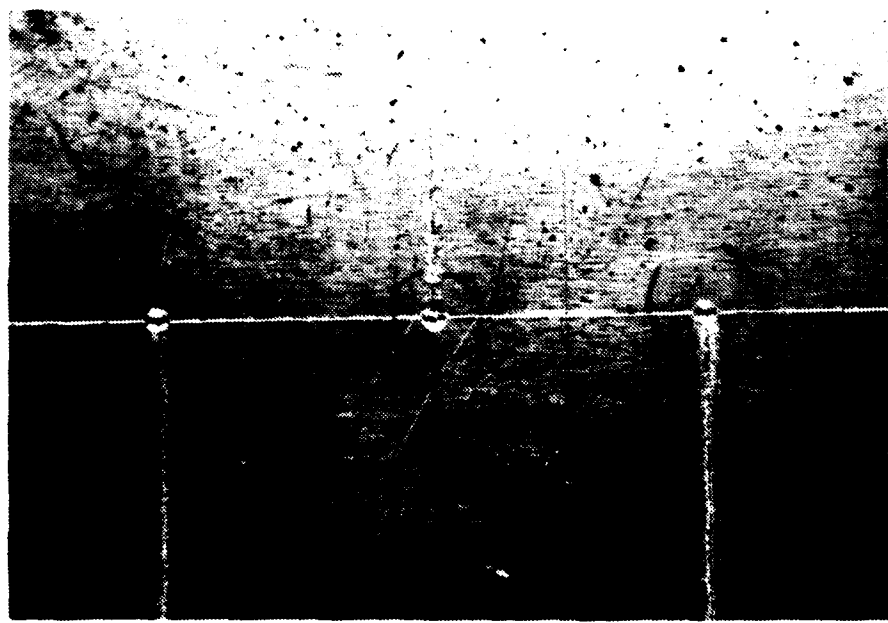


Figure 7. Photograph of Thermocouple Placement Holes.



Figure 8. Photograph of Both Inner Plates Showing Thermocouple Slot Pattern.

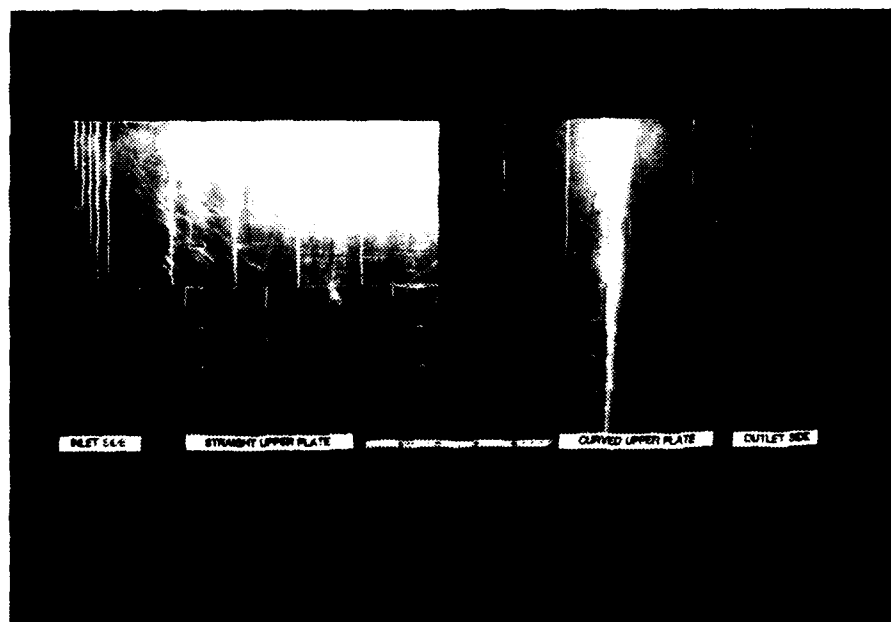


Figure 9. Photograph of Both Outer Plates Showing Thermocouple Slot Pattern.

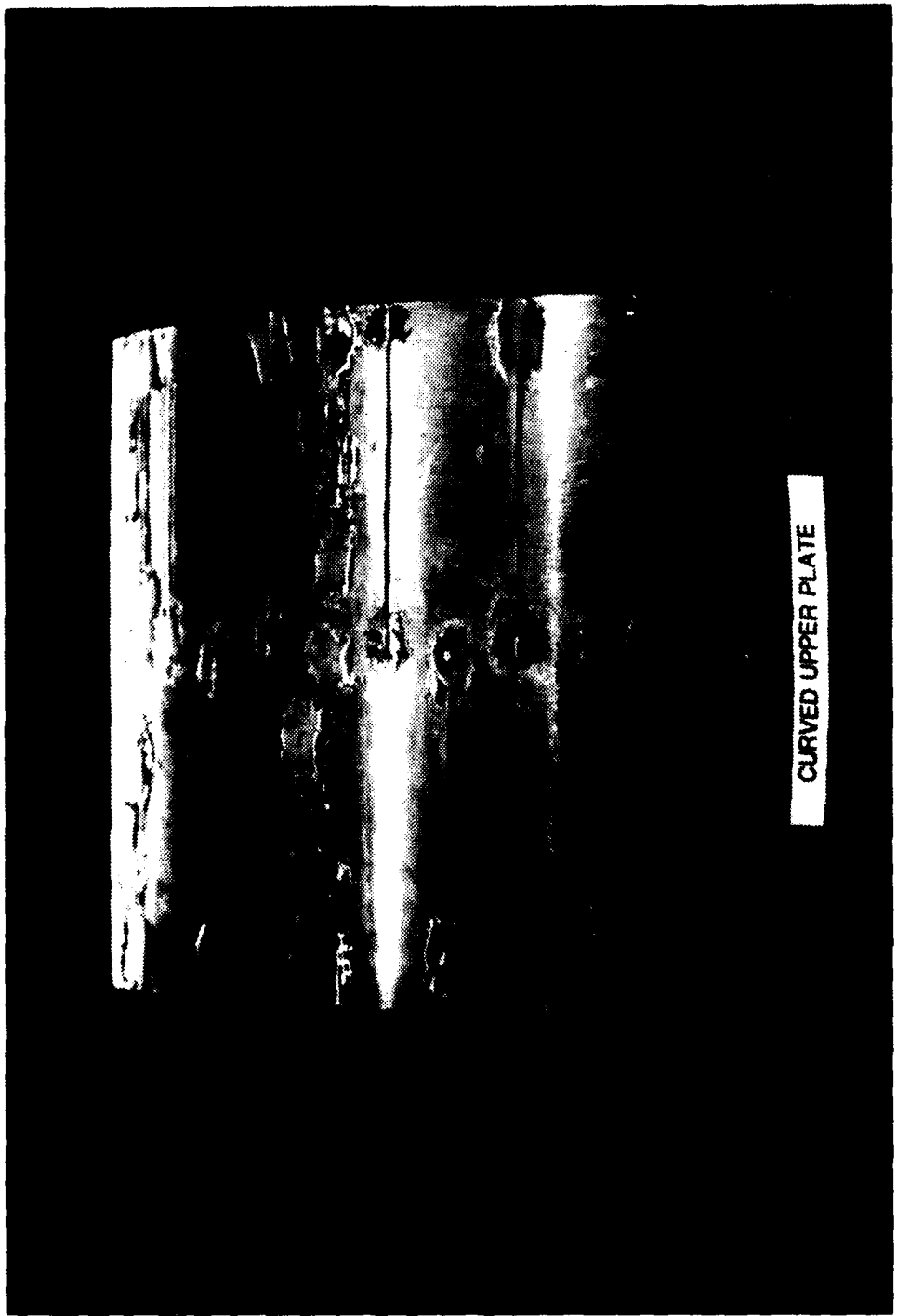


Figure 10. Photograph of Epoxied Thermocouples in Outer Curved Plate.



Figure 11. Photograph of Epoxyed Thermocouples in Outer Straight Plate.



Figure 12. Photograph of Convex Surface of Copper Plate.

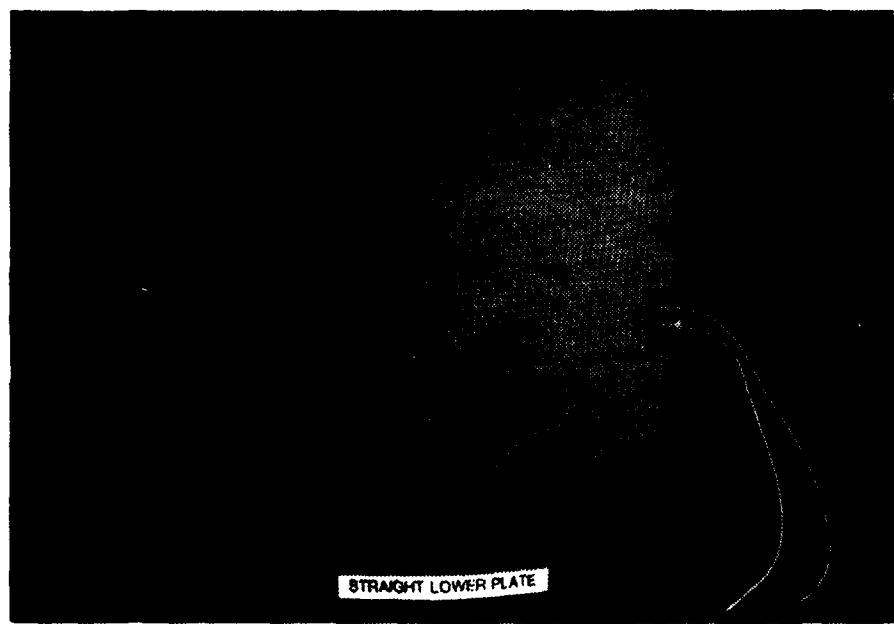


Figure 13. Photograph of Completed Heated Test Section.

by heating and forming the Plexiglas around the wood frame. The Plexiglas wall was secured to the frame by screws tapped into the steel rails. The heated copper sections were then fitted into the machined spaces and two 0.635 centimeter thick and 2.223 centimeter wide Plexiglas spacers, that served as the sides of the channel and support for the copper plates, were attached by screws to the inner wall and steel rails. The two spacers were 25.4 centimeters apart and formed the width of the channel. Additionally, five flat head screws spanning the width of the channel at the joints where the copper and Plexiglas met were used to secure the copper plates and maintain an even joint. The seams were then worked to a smooth transition by applying "Bondo" to the joints and sanding. See Figures 14, 15, 16, and 17.

The outer wall was constructed in a similar manner, but using 0.318 centimeter thick and 29.85 centimeter wide pieces of Lexan. Lexan was used on the outer wall because of its flexibility and ease of bending without heat, which would be required when attaching the outer wall to the inner wall and frame. Also, the outer wall was formed in an outer wood frame so that the transition joints of the outer wall could be worked smooth like the inner wall. See Figures 18 and 19. Both walls were constructed so that no seams or butt joints existed on the inside of the channel, except

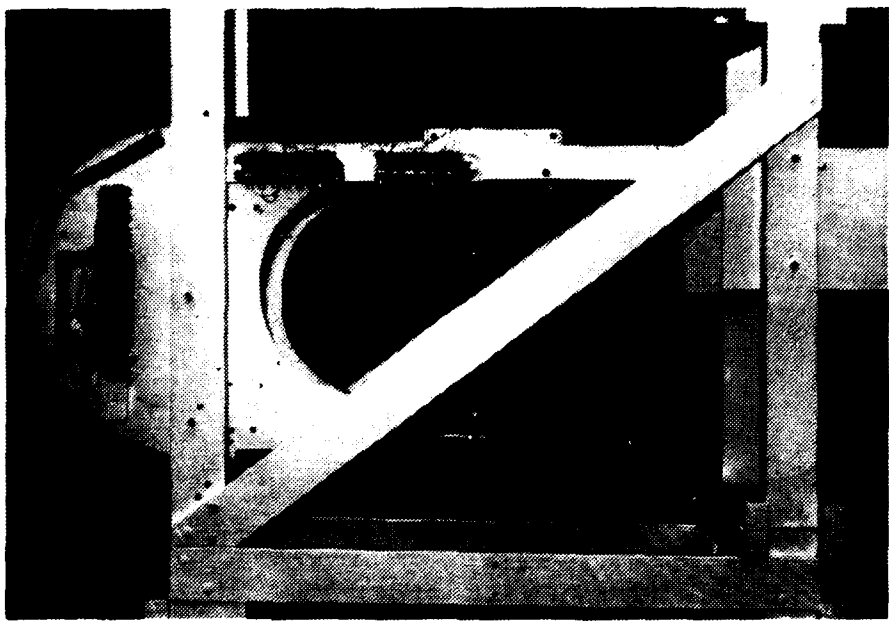


Figure 14. Photograph of Channel Frame.

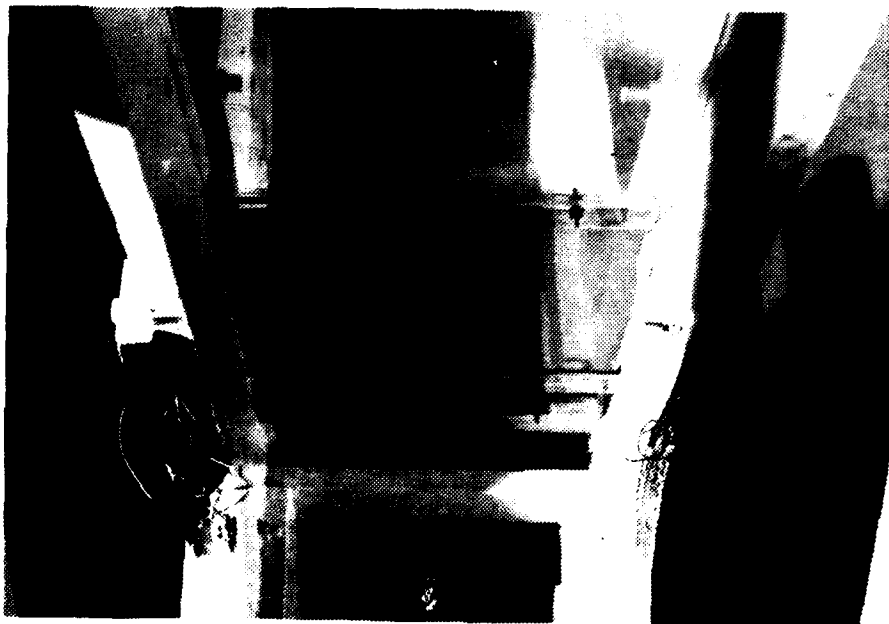


Figure 15. Photograph of Bottom View of Inner Straight Test Section.

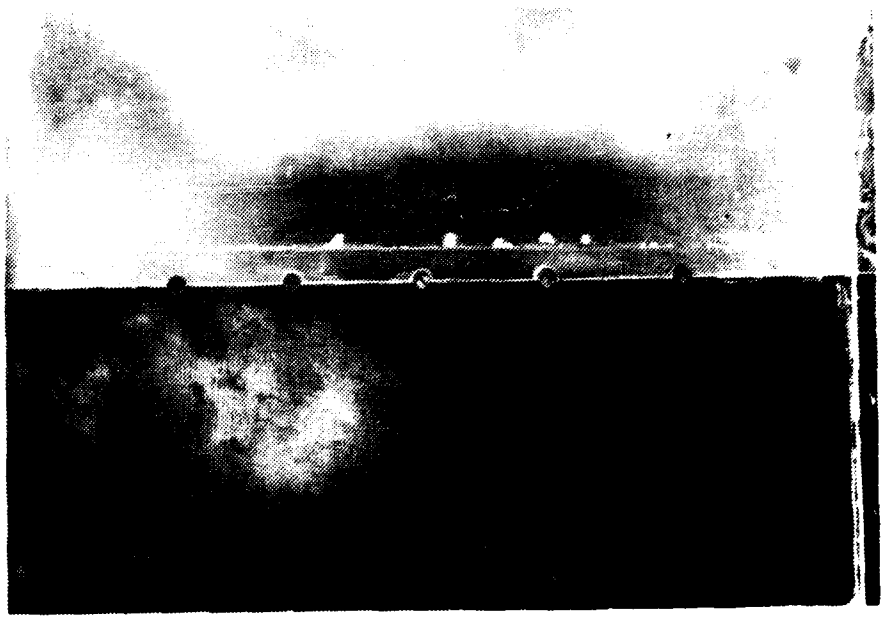


Figure 16. Photograph of Inner Straight Wall at Copper-Plexiglas Joint.



Figure 17. Photograph of Inner Curved Wall at Copper-Plexiglas Joint.



Figure 18. Photograph of Outer Frame and Lexan Wall
Showing Straight Test Section.

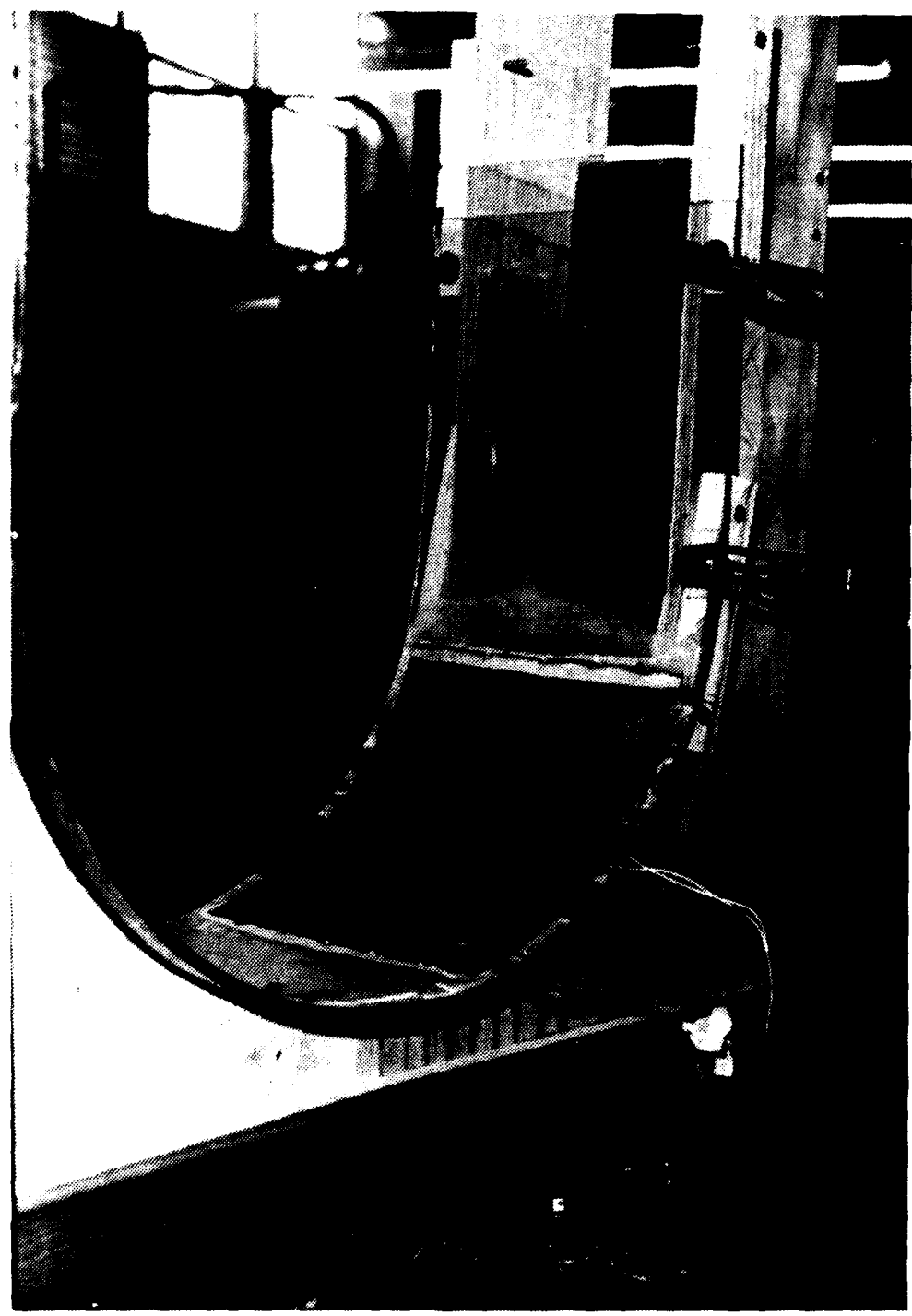


Figure 19. Photograph of Outer Curved Test Section.

where the heated copper section joined the Plexiglas and Lexan walls, and all eight of those joints had a smooth transition.

Once both walls were completed, the outer wall and support frame was positioned onto the inner wall and main frame. The outer wall was aligned onto the inner wall and the outer wall support frame removed. The outer wall was then bolted to the inner wall and frame with steel bars running the length of the channel used as a spacer to insure even compression. Once this was completed the inlet and outlet nozzles were attached to the channel.

The sides of the channel and all connections between the channel, the pvc piping, and the orifice were sealed with Macklanburg-Duncan Silicone Rubber Sealant Caulk to ensure there was no leakage of air into the channel or the piping which could effect the recorded temperatures or mass flow rate. The entire channel was thermally insulated with three layers of 1/2 inch Armstrong Armaflex 22 Sheet Insulation, a flexible foamed plastic material. By positioning thermocouples between these insulation layers, the heat lost through the insulation could be computed at each test section. The heat loss through insulation surrounding the rest of the channel due to the heated air flowing through the channel was a small fraction of the total power supplied to the heater. The insulation was held in place by the use of silver duct tape and velcro strips attached to the frame.

C. INSTRUMENTATION

The data acquisition system used for this experiment was a Hewlett Packard 3054A Automatic Data Acquisition/Control System consisting of a 3456A Digital Voltmeter, a 3497A Data Acquisition/Control Unit, and four input panels capable of reading any mix of eight voltages or copper-constantan thermocouples. Also used in conjunction with this data acquisition system, were a Hewlett Packard 9826 Computer and 2671A Printer. The program used to reduce the data is listed in Appendix A.

The copper-constantan thermocouples were calibrated against a platinum resistance thermometer using a ROSEMONT Commutating Bridge model 920A, and a ROSEMONT Constant Temperature Bath model 913A. All thermocouples were calibrated between 20 and 85 degrees Celsius, and a second order polynomial was curve fitted to correct each thermocouple.

The mass flow rate in the channel was measured with a thin plate orifice measuring device which was placed in the 2 inch pvc piping between the channel and the compressor. In this study an orifice with a diameter of 2.7318 centimeters was used to measure hydraulic Reynold's numbers above 5000. The orifice device was installed in accordance with ASME Power Test Code [Ref. 30], with 3/8 inch pressure taps placed on either side of the orifice at 1 and 1/2

diameters, and one thermocouple inserted in the two inch pvc piping down stream of the orifice to record the temperature of the air flowing through the orifice. Pressure measurements were taken with Meriam vertical manometers, one whose fluid was water with a 0 to 60 inch range, another using water with a 0 to 30 inch range, and a third whose fluid was mercury, calibrated to read inches of water with a range of 0 to 415 inches. Atmospheric pressure was measured with a Princo precision barometer. The pressure readings were used to calculate the mass flow rate of the working fluid as outlined in [Refs. 30, 31].

Power was supplied to the heated test section by using two Lambda Model LK345A FM 60 volt power supplies in series. The power supplies are rated at 6.0 amps. maximum at 40 degrees Celsius. Since the electrical resistance of the rubber heater is not constant, but varies slowly with temperature, a precision resistor was calibrated and connected in series with the heater to allow the calculation of the instantaneous power being supplied. Both the outer and inner heated test sections have their own circuitry and precision resistor. The value of the precision resistor for the outer test sections is 2.0173 ohms, and the value for the inner test sections is 2.0084 ohms. See Figure 20 for diagram of circuit used to measure instantaneous power.

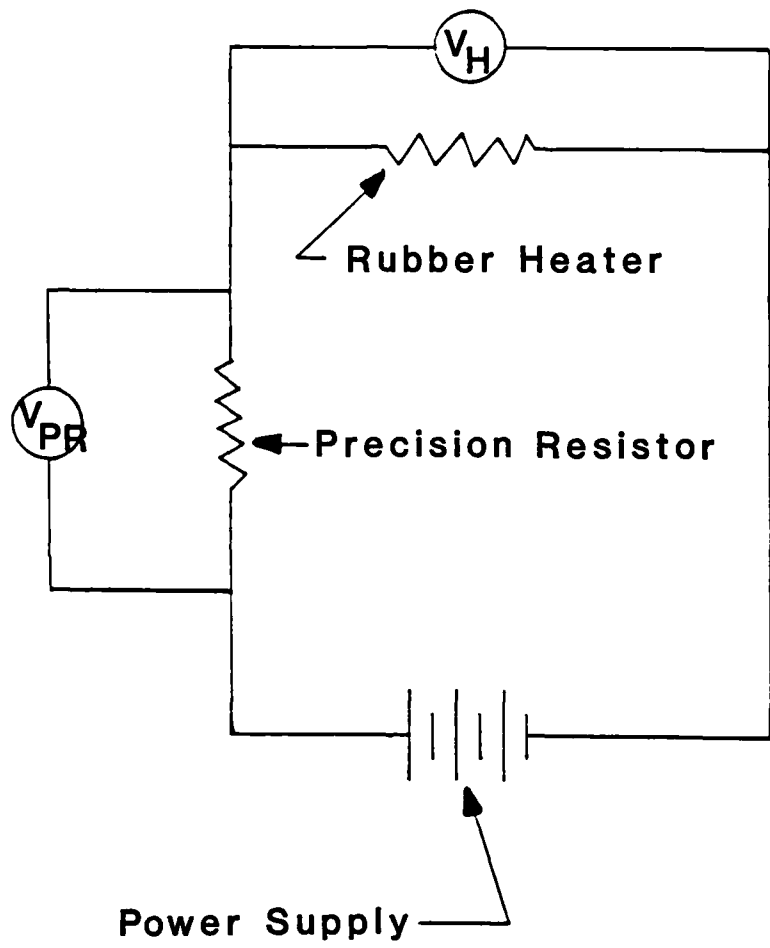


Figure 20. Power Measurement Circuit.

The working fluid was air at room temperature, which was drawn through the channel by an electrically driven Spencer Turbo Compressor, rated at 30 horsepower at 3500 rpm, and 550 cubic feet per minute at 70 degrees fahrenheit and one atmosphere. Photographs of the channel and associated test equipment are shown in Figures 21, 22, 23, and 24.

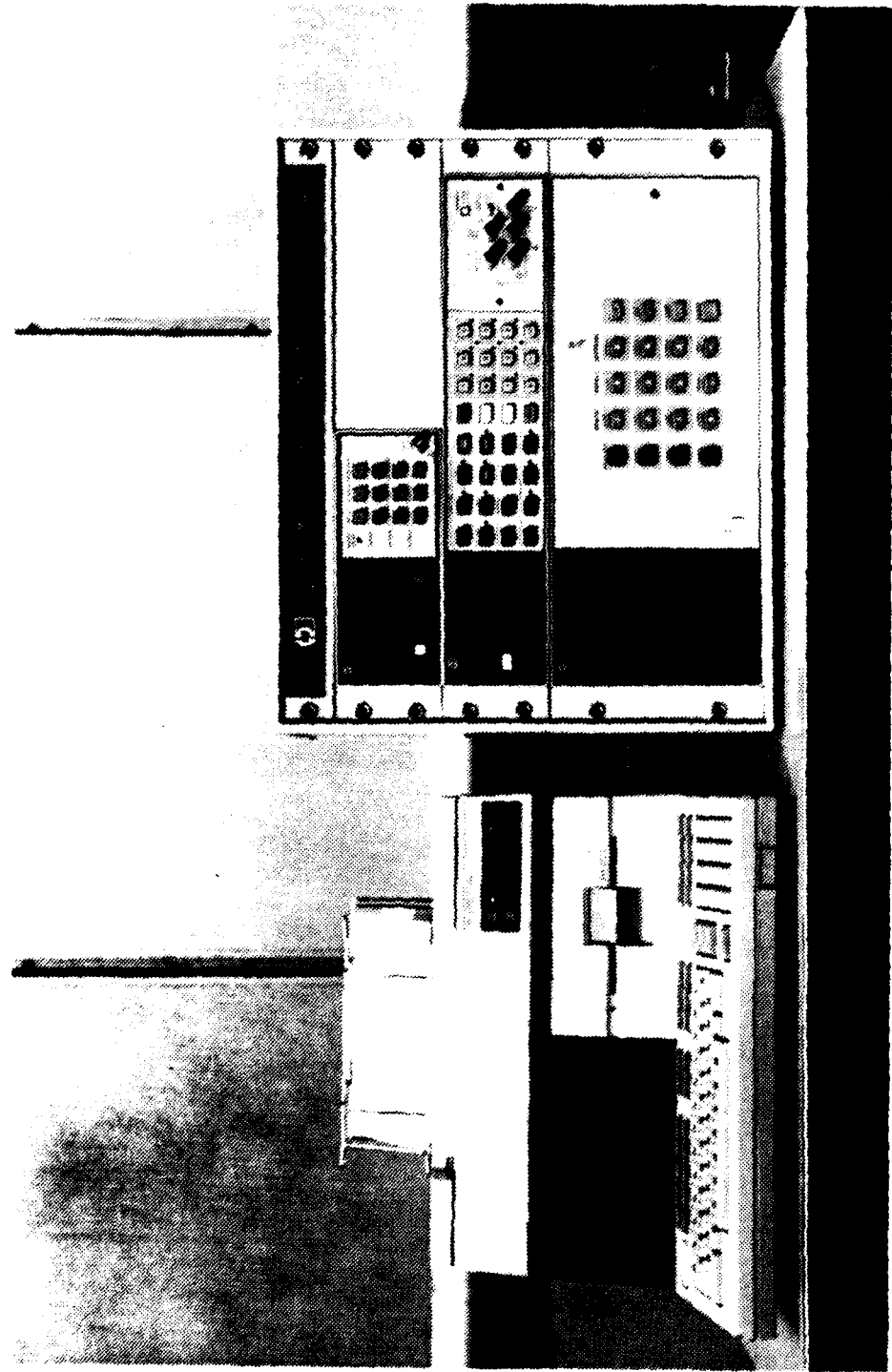


Figure 21. Photograph of Data Acquisition System.

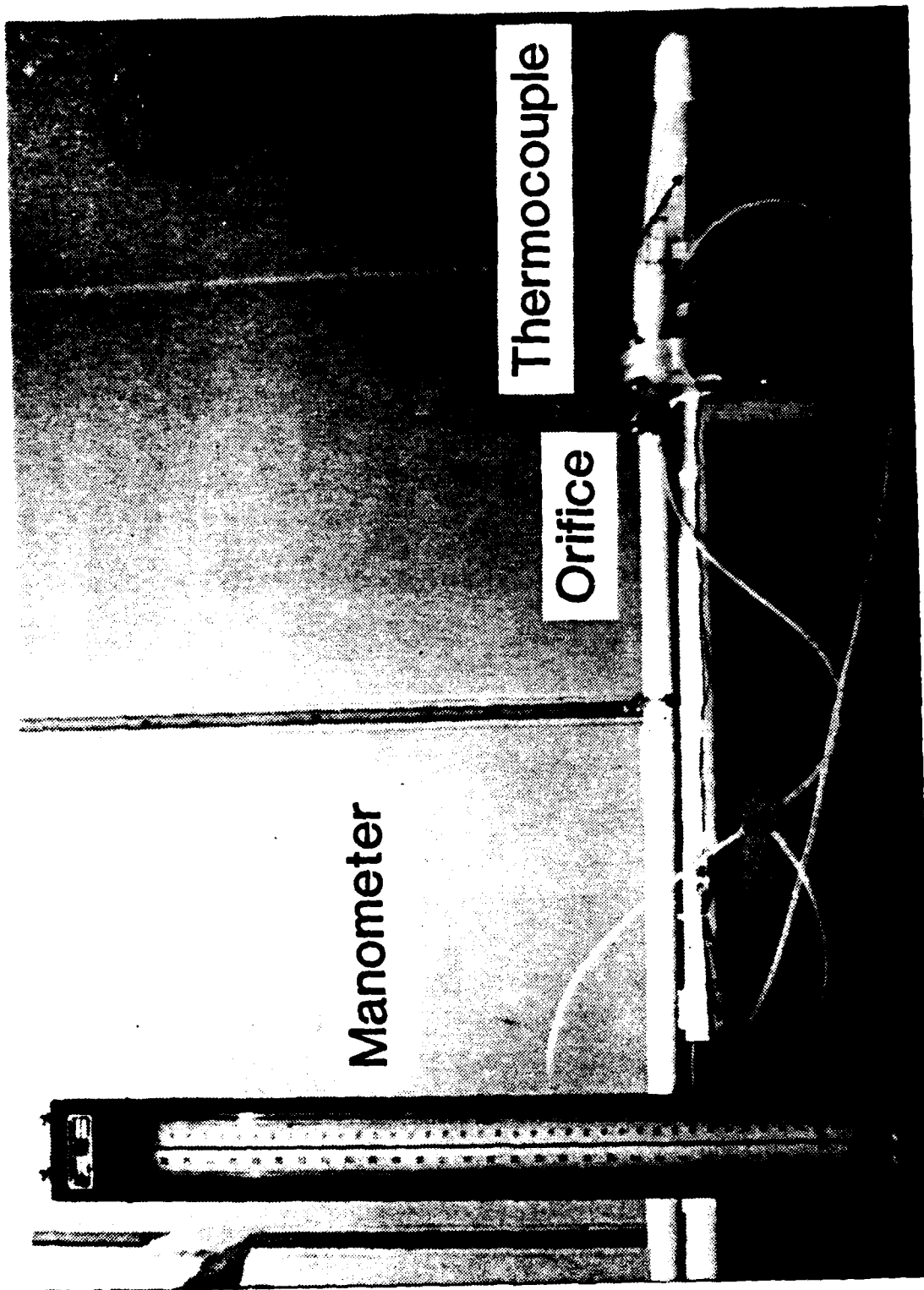


Figure 22. Photograph of Flow Measuring Apparatus.

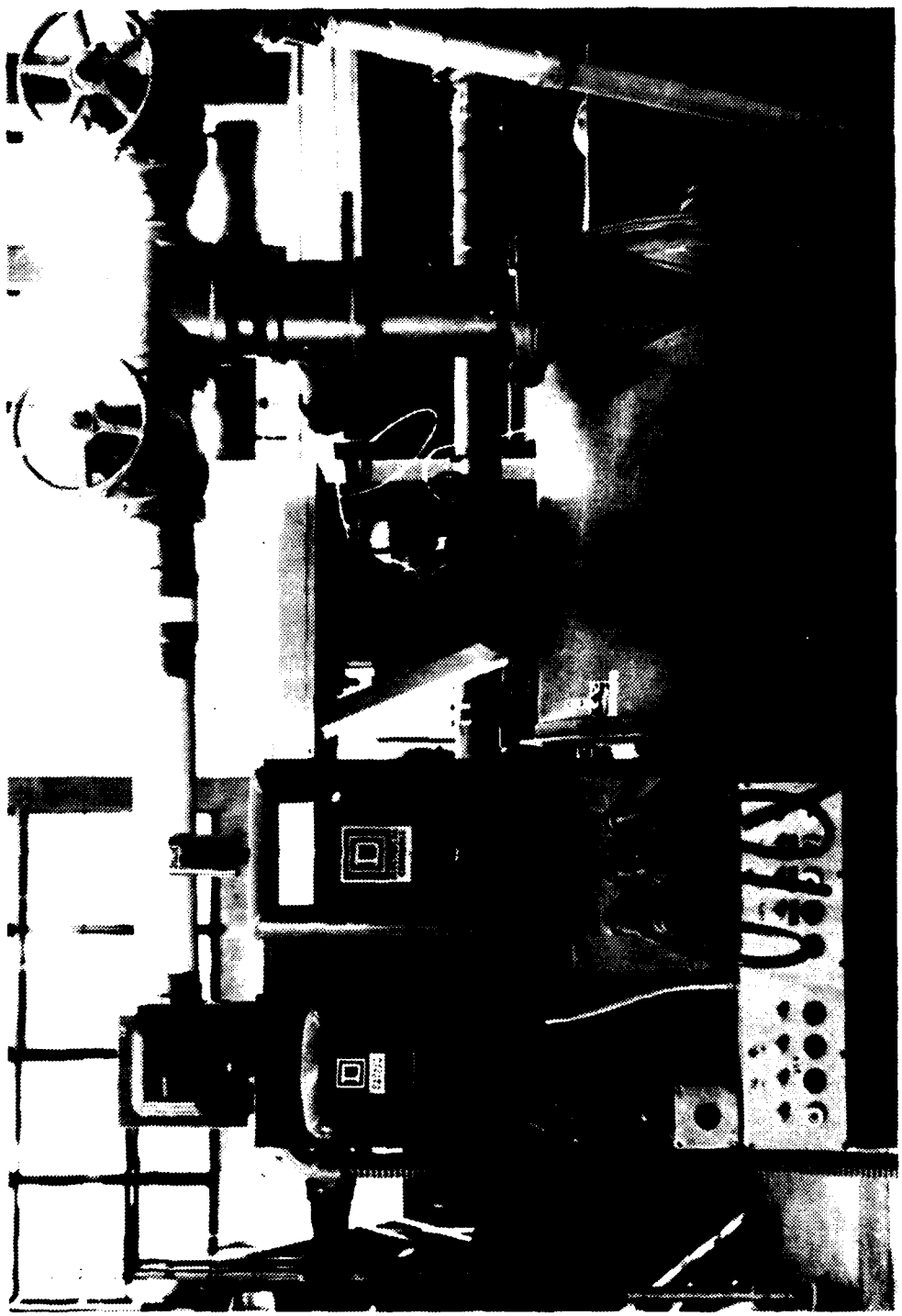


Figure 23. Photograph of Spencer Turbo Compressor.

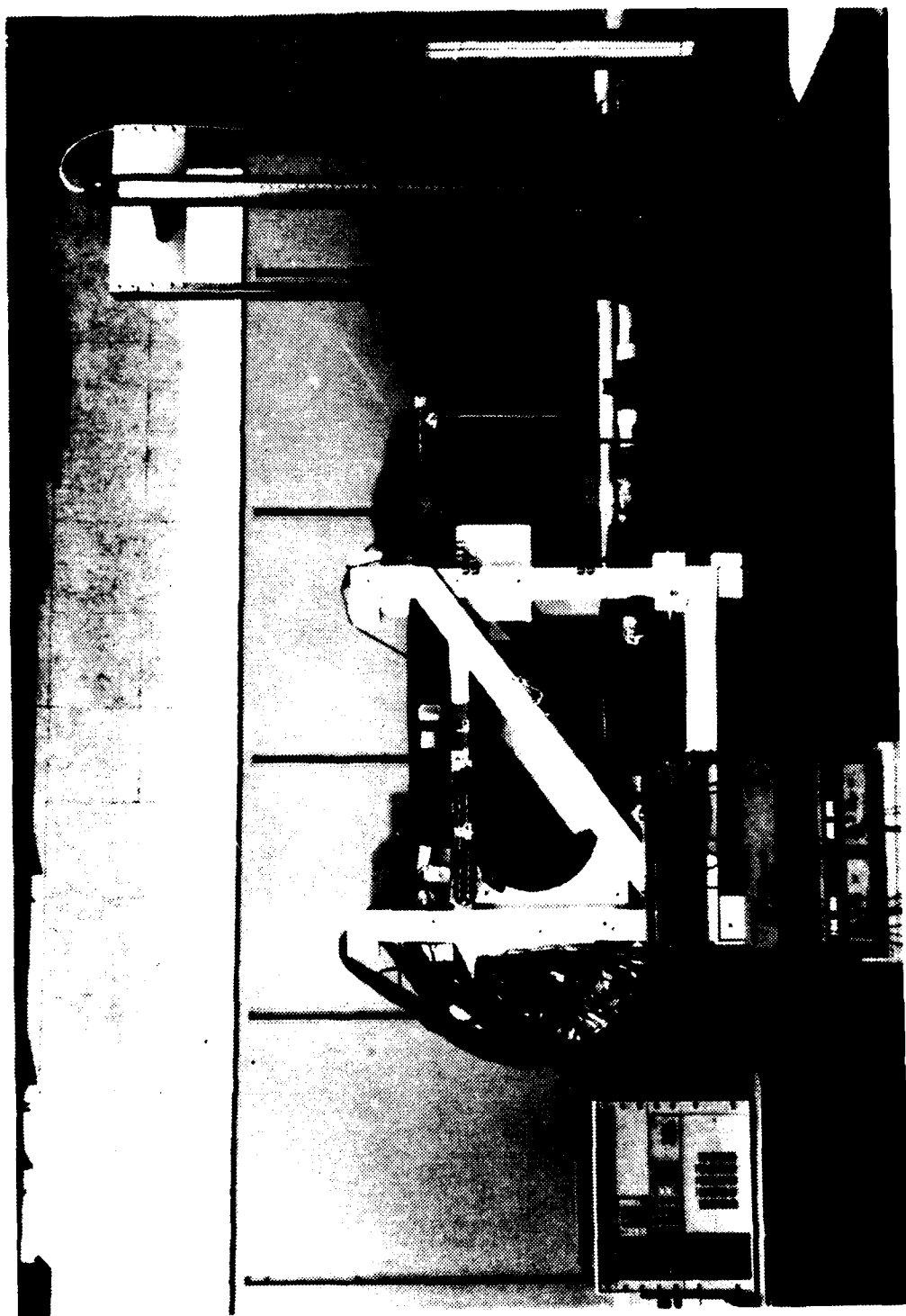


Figure 24. Photograph of Test Channel.

IV. EXPERIMENTAL PROCEDURES

The experimental procedures followed were the same for the straight and curved test sections. The procedure for starting up the experimental apparatus is as follows:

- (1) turn on the computer and data acquisition system
- (2) close globe valve at channel exit
- (3) close valve to manometer reading P_1
- (4) set compressor blast gate to 1/8 open
- (5) start turbo compressor
- (6) open intake valve on compressor 1/4 to 1 turn
- (7) open globe valve at channel
- (8) open manometer valve slowly to ensure P_1 does not exceed manometer scale
- (9) turn on and adjust power supply to the heater
- (10) use intake valve on compressor to control mass flow rate through the channel

It was necessary to determine the approximate voltage setting required to bring the heated wall to approximately 50 degrees Celsius. This heated wall temperature would ensure a large temperature difference between the inlet and outlet temperatures, and the heated and unheated wall temperatures, while not damaging the apparatus. The larger the temperature difference the smaller the uncertainty in the results. The required power setting was found by

monitoring the heated plate temperature locally from the data acquisition system while the voltage to the heater was adjusted.

To compute the instantaneous power supplied to the heater the following relationship was used:

$$Q_p = \frac{V_h V_{PR}}{R_{PR}}$$

The precision resistor voltage and the heater voltage were read by the data acquisition system and the resistance of the precision resistor was a known constant. A diagram of the circuit used was shown in Figure 16.

The mass flow rate was monitored by the two manometers at the orifice. For each run, the atmospheric pressure, the pressure difference across the orifice, and the pressure upstream of the orifice were entered manually into the computer for the mass flow rate calculation. All other data was acquired by the data acquisition system directly from the experimental apparatus.

Once the apparatus was started properly, sufficient time was required to reach steady state prior to gathering data. Preliminary runs were performed to determine the time required for the test apparatus to reach steady state. For this experiment at least two hours were allowed for a cold test apparatus to reach steady state, and at least one hour

if the apparatus was already running. After waiting the required time, data was taken at ten minute intervals to ensure that a steady state condition had been achieved. The criteria for steady state was based on three variables:

- (1) the difference between inlet and outlet temperature
- (2) the heated test section wall temperature
- (3) the unaccounted heat loss in the system

When the first two of these quantities varied by less than two percent over a ten minute interval and the third was less than ten percent of the input power, it was considered that a steady state condition had been achieved.

Experiments were conducted at specific mass flow rates of air corresponding to Reynolds numbers between 7000 and 22000. The Reynolds number was based on the hydraulic diameter of the channel. For each mass flow rate, temperature and voltage data were taken automatically by the data acquisition system and immediately reduced and printed. The variables that were measured and used in this investigation were:

- (1) the temperature of the air entering the channel (T_{in})
- (2) the temperature of the air leaving the channel (T_{out})
- (3) the temperature of the heated wall in the test section (T_{wo} or T_{wi})
- (4) the temperature of the unheated wall in the test section (T_{wi} or T_{wo})
- (5) the temperature between each layer of insulation at the test section (T_{ins})

- (6) the temperature of the air at the orifice (T_{orf})
- (7) the voltage across the precision resistor (V_{PR})
- (8) the voltage across the rubber heater (V_H)
- (9) the pressure upstream of the orifice (P_1)
- (10) the difference in the upstream and downstream pressure across the orifice (ΔP)
- (11) the atmospheric pressure (P_{ATM})

The results obtained from the straight test sections served as a baseline for the comparison of the curved section results. An effort was made to match the mass flow rates for each test section as closely as possible.

V. PRESENTATION OF DATA

A. DATA REDUCTION

The constant heat flux surface for the heated wall of each test section was provided by the uniform electrical resistivity of the rubber heater. The insulated unheated wall was considered adiabatic since the heat losses through that wall were negligible. The straight portion of the channel upstream of the straight heated test section was of sufficient length to ensure that the air flow was hydrodynamically fully developed for the flow velocities of this experiment. The straight portion of the channel downstream of the curved section proved to be of sufficient length to ensure that the air flow exiting the channel was thoroughly mixed and that the measured outlet air temperature (T_{out}) was an average bulk temperature, as long as the hydraulic Reynolds number of the channel was less than 17000.

The analysis of the data required several quantities to be defined. The heat convected to the air was calculated using the equation:

$$Q_{air} = \dot{m}C_{pair} (T_{out} - T_{in})$$

where ' C_{pair} ' is the specific heat of the air at constant pressure and ' \dot{m} ' is the mass flow rate of the air.

The average heat transfer coefficient between the heated wall and the flow of air in the channel was defined by the equation:

$$\bar{h} = \frac{Q_{air}}{A_{PL} \Delta T}$$

where ' Q_{air} ' is defined above, ' A_{PL} ' is the area of the heated copper plate in the test section, and ' ΔT ' is the difference between the arithmetic average heated wall temperature (T_w) and the average bulk air temperature (T_{blk}). The average bulk air temperature is defined as the arithmetic mean of the entrance and exit air temperatures (T_{in} , T_{out}).

The average Nusselt number was then calculated using:

$$\bar{Nu}_{hd} = \frac{\bar{h} D_{hd}}{K_{air}}$$

In this equation ' D_{hd} ' is the hydraulic diameter and ' K_{air} ' is the thermal conductivity of the air.

The hydraulic Reynolds number was calculated for each test run as follows:

$$Re_{hd} = \frac{\dot{m} D_{hd}}{A_c \mu_{air}}$$

where again ' \dot{m} ' and ' D_{hd} ' are the mass flow rate and hydraulic diameter of the channel, ' A_c ' is the cross-

sectional area of the channel, and ' μ_{air} ' is the dynamic viscosity of the air.

For the curved sections the Dean number was defined as:

$$D_e = \frac{\dot{m} D_c / 2}{A_c \mu_{air}} \sqrt{\frac{D_c / 2}{R_i}} = \frac{Re_d}{2} \sqrt{\frac{D_c / 2}{R_i}}$$

where ' Re_d ' is the Reynolds number based on the channel height, ' D_c ' is the channel height, and ' R_i ' is the radius of curvature of the inner convex wall.

A sketch of the control volume and a set of sample calculations for one test run of the curved section are given in Appendix B. A sample calculation for the uncertainty analysis is given in Appendix C.

B. RESULTS

The data obtained from each experimental run was reduced by the computer program listed in Appendix A, utilizing the expressions described in Part A above. The major parameters resulting from this process are shown in Tables I through IV. Tables I and II contain the straight sections results and Tables III and IV contain the results of the curved sections. A plot of the average Nusselt number versus hydraulic Reynolds number is given in Figures 25, 26, 27, 28, and 29 for the comparison of the results. "Error" bands have been indicated as a result of the uncertainty analysis.

TABLE I
SUMMARY OF STRAIGHT OUTER WALL TEST RESULTS

Re_{hd}	Q_{air}^r (W)	\bar{h} (W/mC)	ΔT (C)	\bar{Nu}_{hd}
7709	108.50	41.99	28.52	20.07
11953	135.26	61.57	25.49	29.51
15646	157.92	74.43	24.45	35.65
21455	217.53	87.42	27.36	41.95

Reynolds number and Nusselt number are based on hydraulic diameter. Results for Reynolds number of 21455 based on orifice air temperature instead of outlet air temperature.

TABLE II
SUMMARY OF STRAIGHT INNER WALL TEST RESULTS

Re_{hd}	Q_{air} (W)	\bar{h} (W/m°C)	ΔT (C)	\bar{Nu}_{hd}
7628	105.57	41.52	28.90	19.85
12169	138.36	59.50	27.42	28.50
15788	159.84	70.24	26.37	33.61
21312	204.42	81.82	27.84	39.17

Reynolds number and Nusselt number are based on hydraulic diameter. Results for Reynolds number of 21312 based on orifice air temperature instead of outlet air temperature.

TABLE III
SUMMARY OF CURVED CONCAVE WALL TEST RESULTS

Re_{hd}	De	Q_{air} (W)	\bar{h} (W/mC)	T (C)	\overline{Nu}_{hd}
7782	206	115.88	52.43	25.51	25.00
11726	311	157.45	68.16	29.91	32.53
15813	419	158.17	83.13	22.34	39.78
21246	563	231.31	93.02	27.20	44.52

Reynolds number and Nusselt number are based on hydraulic diameter. Results for Reynolds number of 21246 based on orifice air temperature instead of outlet air temperature.

TABLE IV
SUMMARY OF CURVED CONVEX WALL TEST RESULTS

Re_{hd}	De	Q_{air} (W)	\bar{h} (W/m°C)	ΔT (C)	\bar{Nu}_{hd}
7757	206	82.37	38.33	24.47	18.37
12021	318	115.50	57.62	23.92	27.65
15908	421	142.54	68.57	24.34	32.94
21603	572	164.08	79.28	23.43	38.11

Reynolds number and Nusselt number are based on hydraulic diameter. Results for Reynolds number of 21603 based on orifice air temperature instead of outlet air temperature.

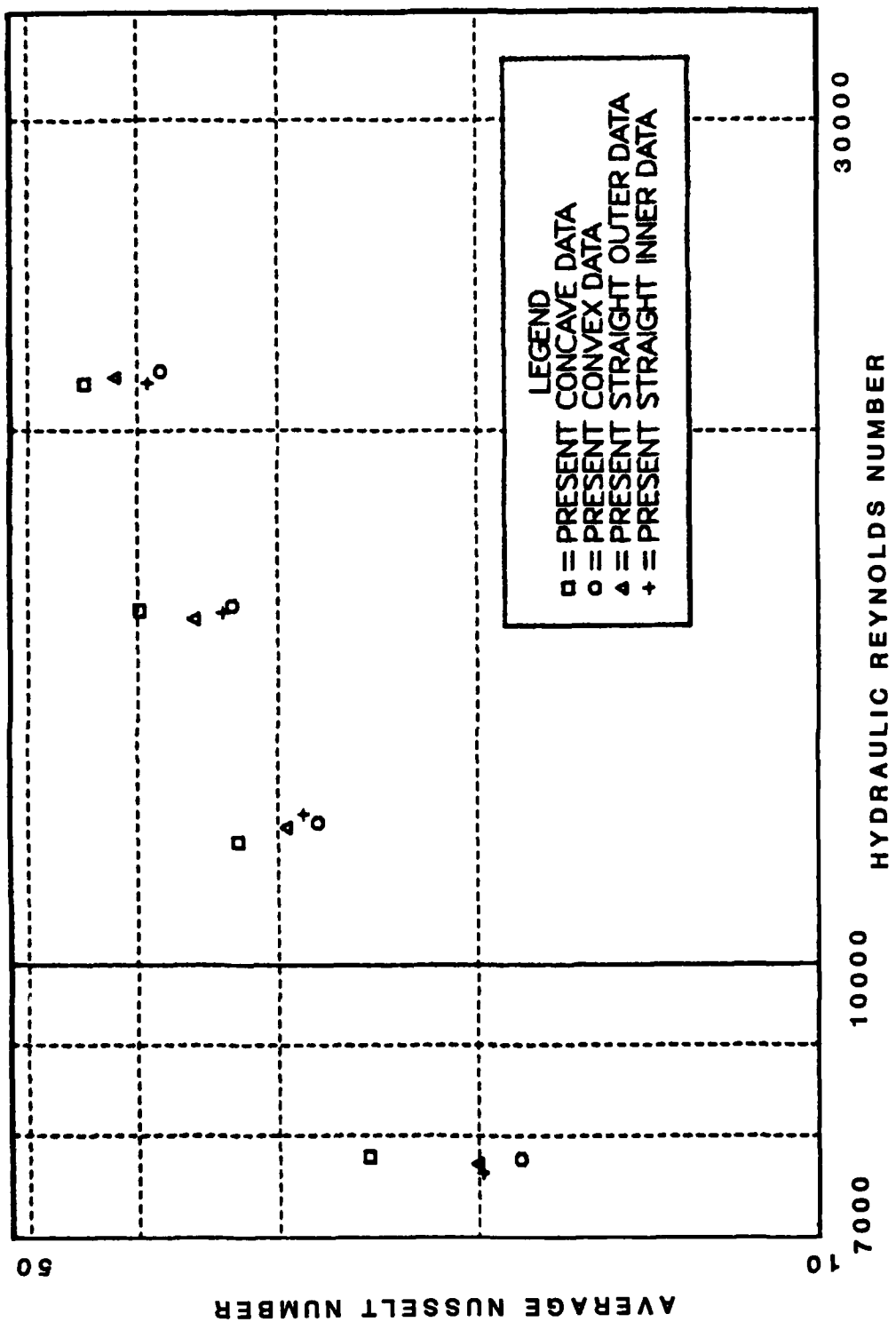


Figure 25. Present Straight vs. Curved Section Results.

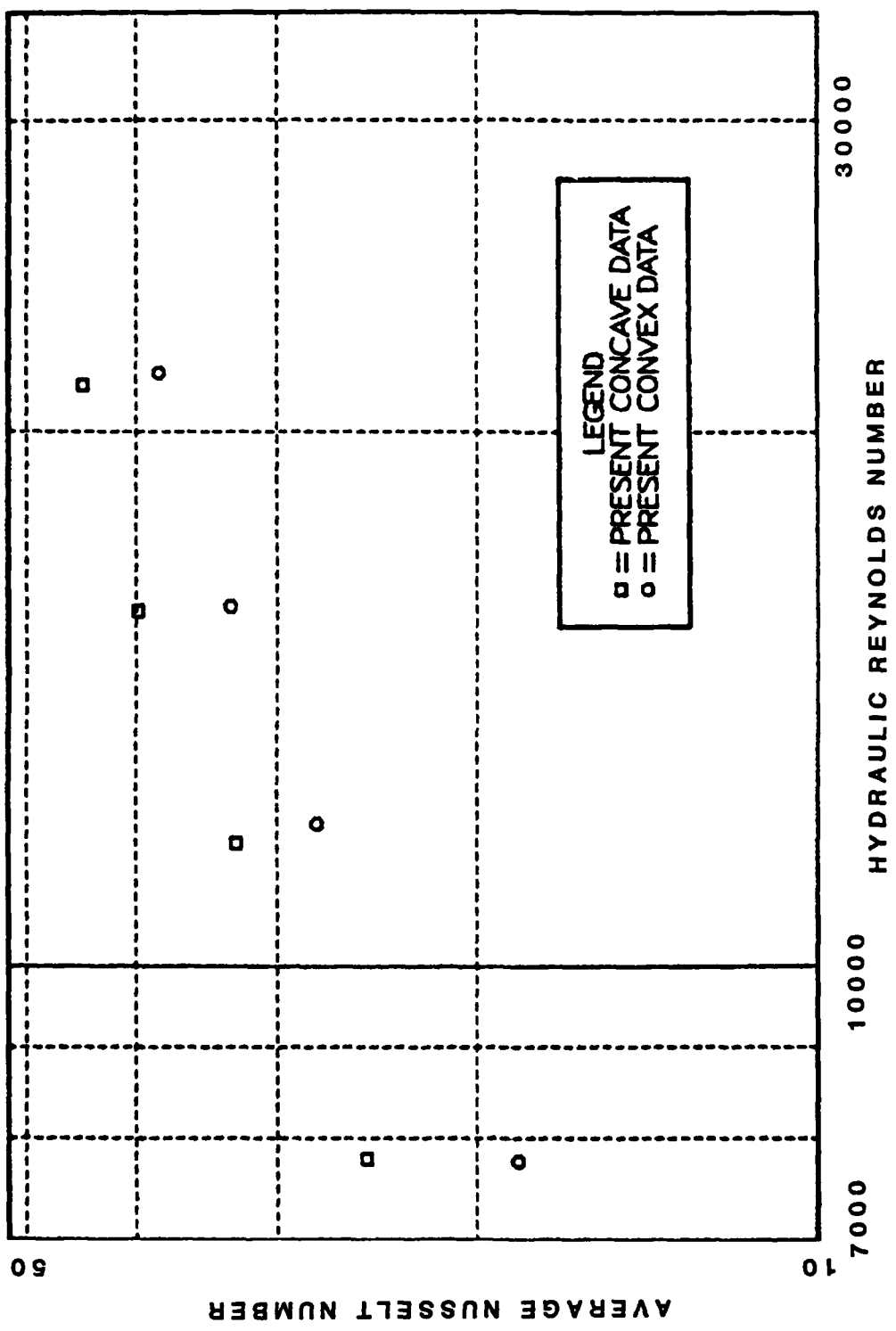


Figure 26. Present Concave vs. Convex Section Results.

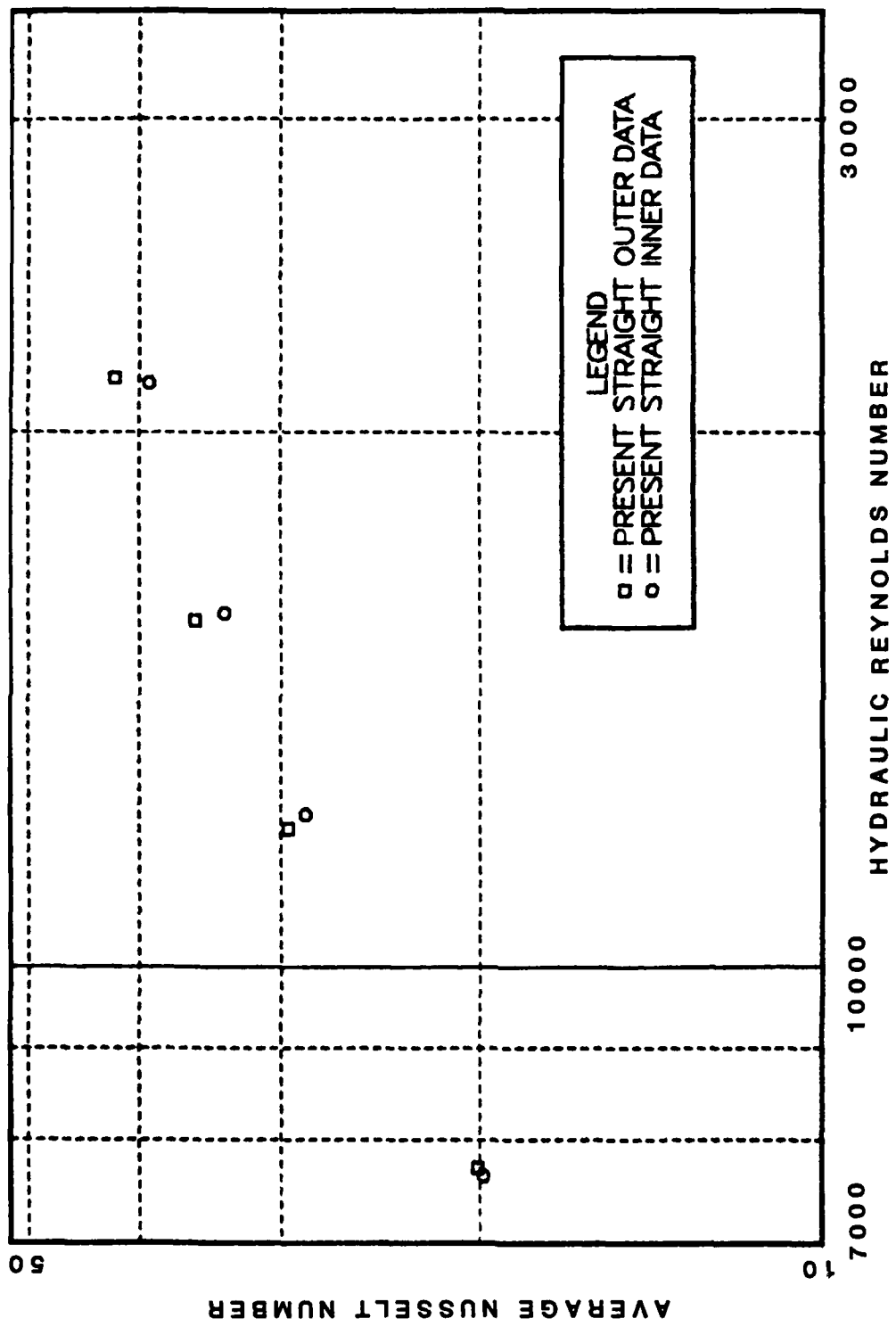


Figure 27. Present Straight Outer vs. Inner Section Results.

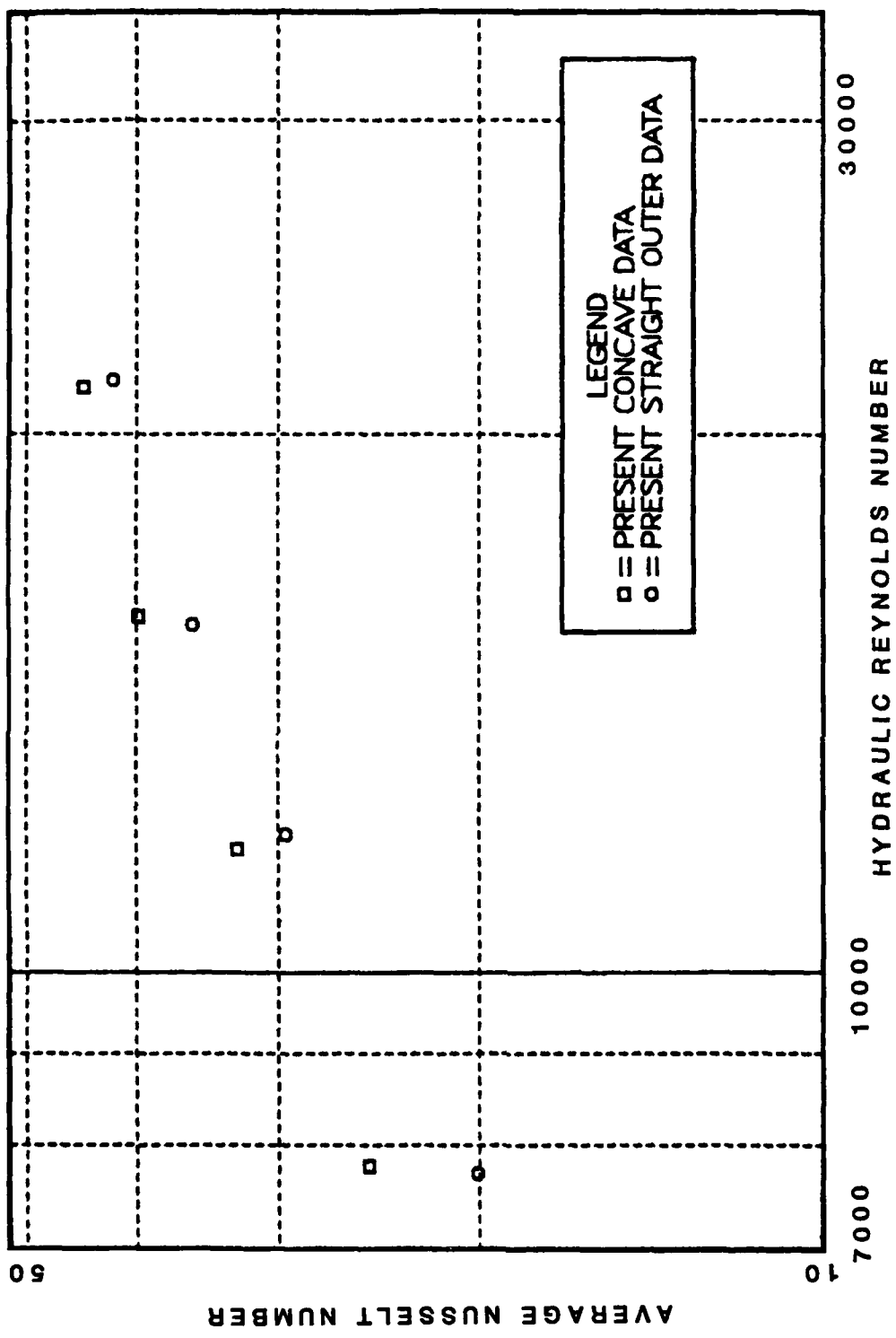


Figure 28. Present Concave vs. Straight Outer Section Results.

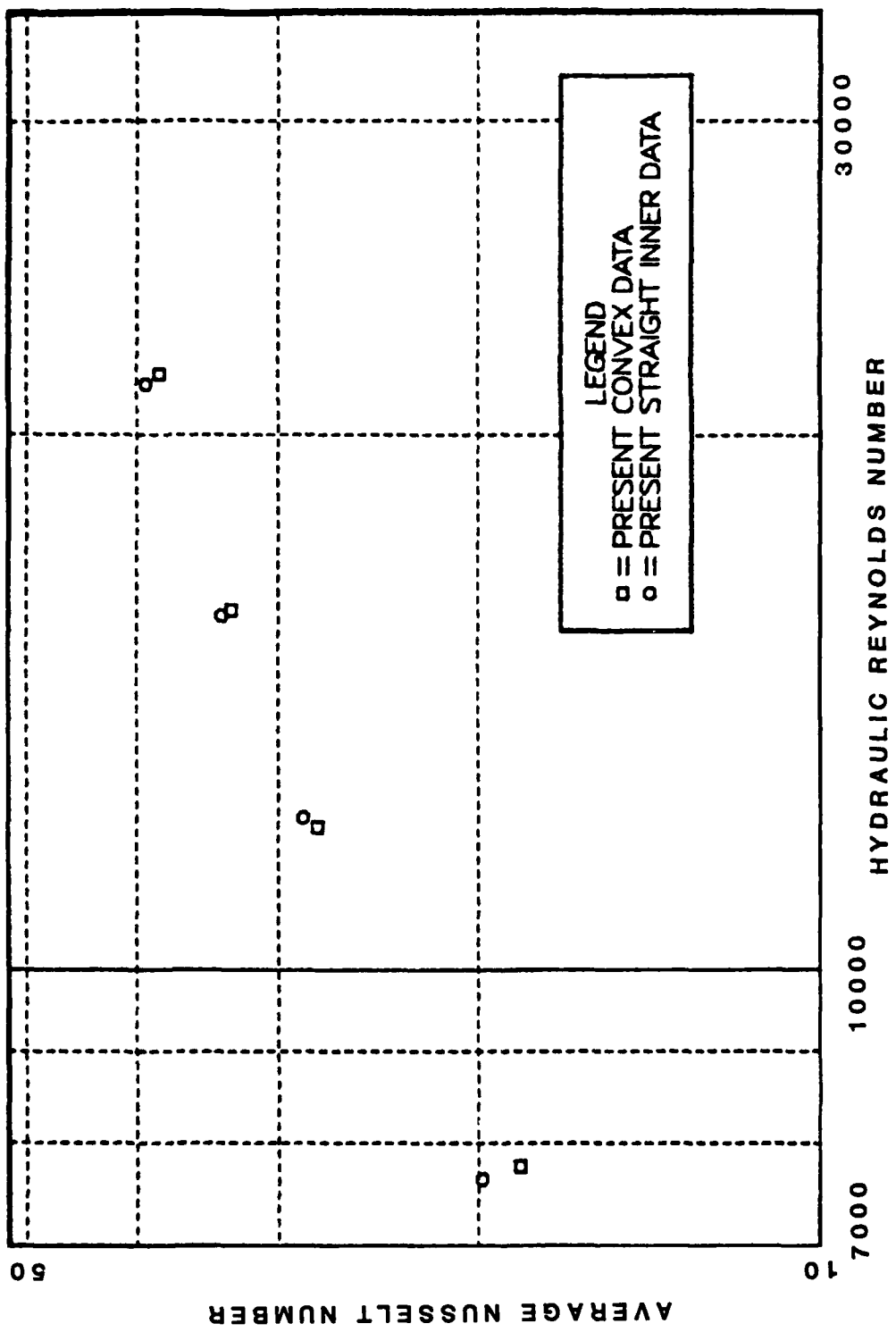


Figure 29. Present Convex vs. Straight Inner Section Results.

As would be expected the results indicate an increase in the rate of heat transfer with increasing Reynolds number for both the straight and curved test sections. In addition, the heat transfer rate was highest in the concave curved section for each Reynolds number investigated, and lowest in the convex curved section.

In the low end of the turbulent regime, at a hydraulic Reynolds number of 7780, the rate of heat transfer was about twenty-two percent higher in the concave curved section than the outer straight section. As the hydraulic Reynolds number continued to increase, between 11700 and 15800, the rate of heat transfer was approximately eleven percent higher between the concave curved section and the outer straight section. At a hydraulic Reynolds number of 21000 the difference in heat transfer rate decreased to about seven percent.

The results obtained at a hydraulic Reynolds number of 21000 have a much larger uncertainty, because the orifice air temperature was higher than the average outlet air temperature. This signifies that the air was not fully mixed at the outlet, because no heat is added to the air after the outlet air temperature is read, yet the air temperature increased. For hydraulic Reynolds numbers greater than about 17000 the channel outlet section is not long enough to allow the air to mix properly.

The values obtained for the hydraulic Reynolds number of approximately 21000 are based on the orifice air temperature vice the outlet air temperature. This resulted in a Nusselt number higher than obtained by using the the outlet air temperature, but still lower than the actual Nusselt number, because of the small heat loss between the outlet nozzle and the thermocouple at the orifice. This heat loss cannot be accounted for and the temperature used as an outlet air temperature was still lower than the actual outlet air temperature.

In comparing the concave curved wall to the convex curved wall the rate of heat transfer was about thirty-six percent higher in the concave section for a hydraulic Reynolds number of 7780. For hydraulic Reynolds numbers between 11700 and 15800 the rate of heat transfer was twenty percent higher in the concave section, and at a hydraulic Reynolds number of 21200 the rate of heat transfer was seventeen percent higher.

VI. DISCUSSION AND CONCLUSIONS

J. Wilson [Ref. 28], in his study, reported that the actual presence of Taylor-Gortler vortices were verified by the observation of the liquid crystal isotherm distribution in the curved test section. He further reported, that at low values of hydraulic Reynolds number and through most of the transition regime, liquid crystal bands were oriented in the streamwise direction. As the Reynolds number increased turbulent forces began to dominate in the curved section and less evidence could be detected for the existence of the vortices.

The high aspect ratio of the channel provided the basis for the assumption that the experimental apparatus should behave like infinite parallel plates. Holihan's data [Ref. 26] tended to verify this assumption. His experimental data in the laminar flow region, approached the theoretical limit for average Nusselt number for parallel plates with one wall heated at a constant heat flux and the opposite wall adiabatic [Ref. 32]. Based on the assumptions mentioned above, comparisons were made with other analytical and experimental results that were of the same or similar problems.

A comparison of the experimental results of this study and the experimental results of Daughety [Ref. 27] and

Wilson [Ref. 28] are shown in Figure 30 for the curved section, and Figure 31 for the straight section. The channel aspect ratio was 40 for each of these studies and the experimental procedures were similar, with the exception of a slight modification in Wilson's procedures. Wilson [Ref. 28] made a correction to determine the temperature drop across the liquid crystal sheet covering the heated wall. By applying this temperature drop to the measured temperature, the true temperature of the heated wall would be known. After reviewing Wilson's data and experimental procedure it was detected that Wilson was over estimating the temperature drop across the liquid crystal by approximately five to seven percent, and this lead to an over estimation of T of ten to twelve percent. This resulted in an over estimation of the average heat transfer coefficient and the average Nusselt number of between ten and twelve percent. When Wilson's data is lowered by ten percent, both his data and Daughety's data fall within the uncertainty bands of the present study as shown in Figures 32 and 33. Differences were attributed to the inability to account for all of the heat transfer processes and the limitations inherent in any experimental work.

Ballard [Ref. 25] reported an increase in the rate of heat transfer between a concave wall and a straight outer wall of eleven percent for laminar flows. Holihan [Ref. 26] reported an increase of fifteen percent for laminar flows

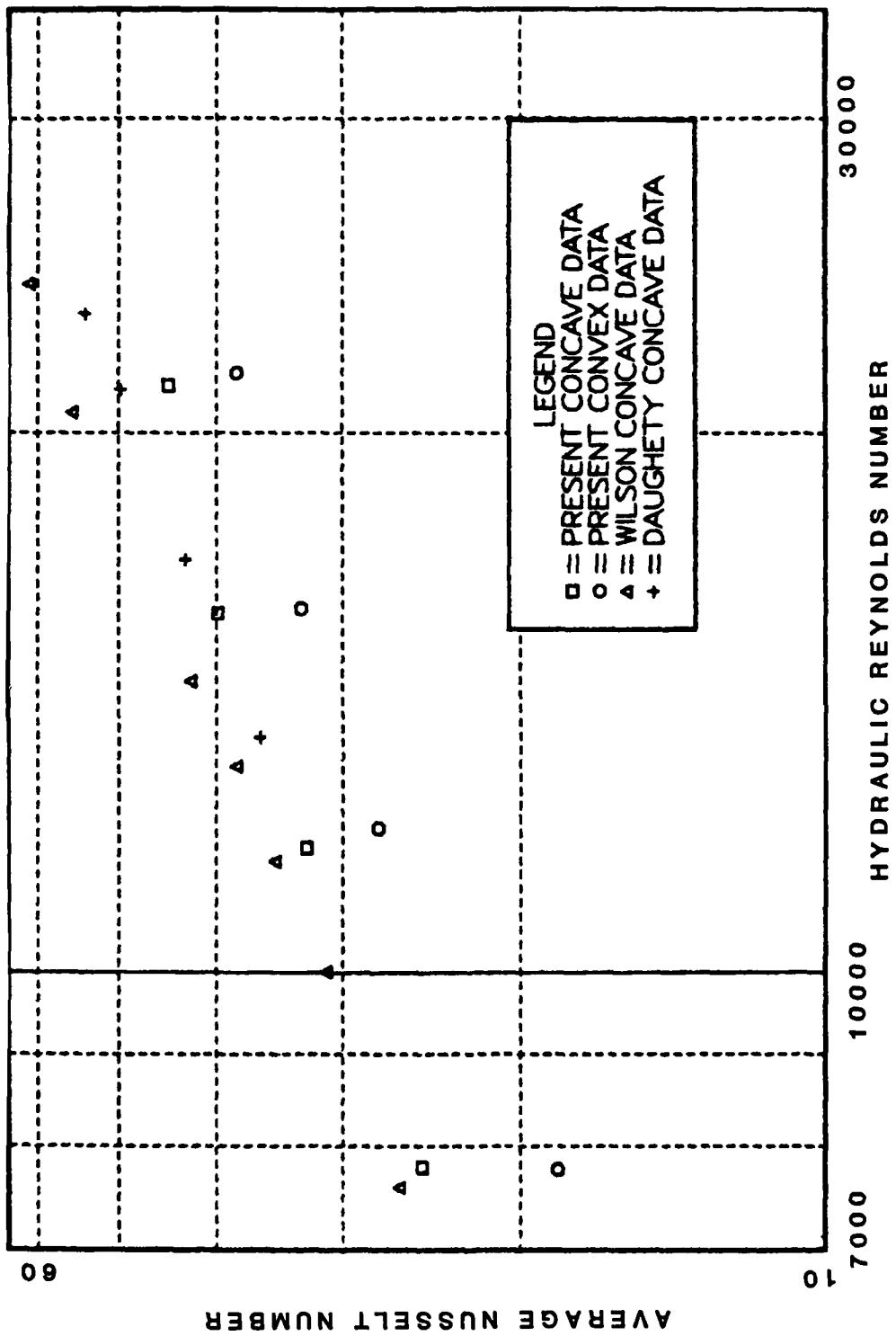


Figure 30. Comparison of Present Data with Daughety and Wilson, Curved Section.

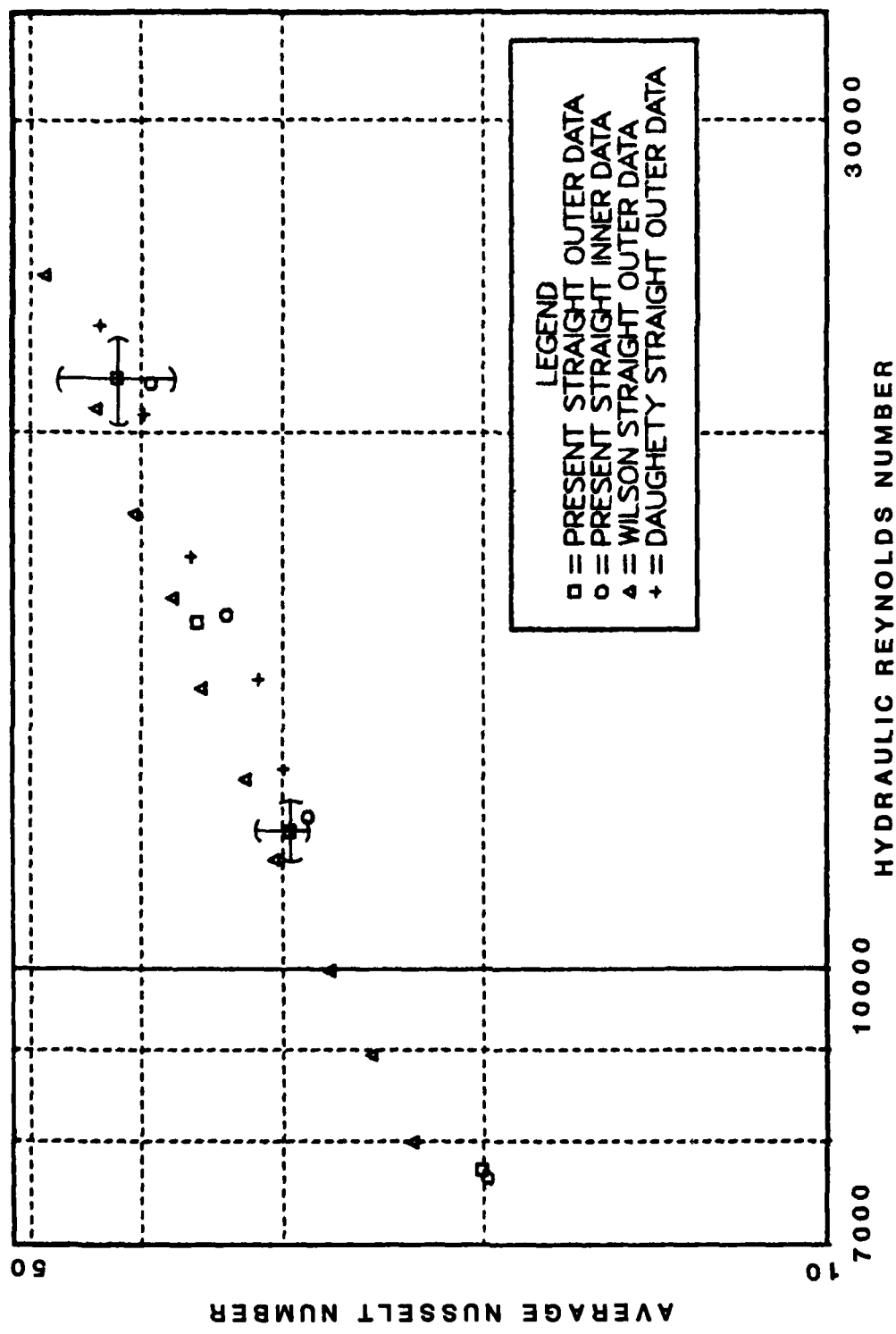


Figure 31. Comparison of Present Data with Daughety and Wilson, Straight Section.

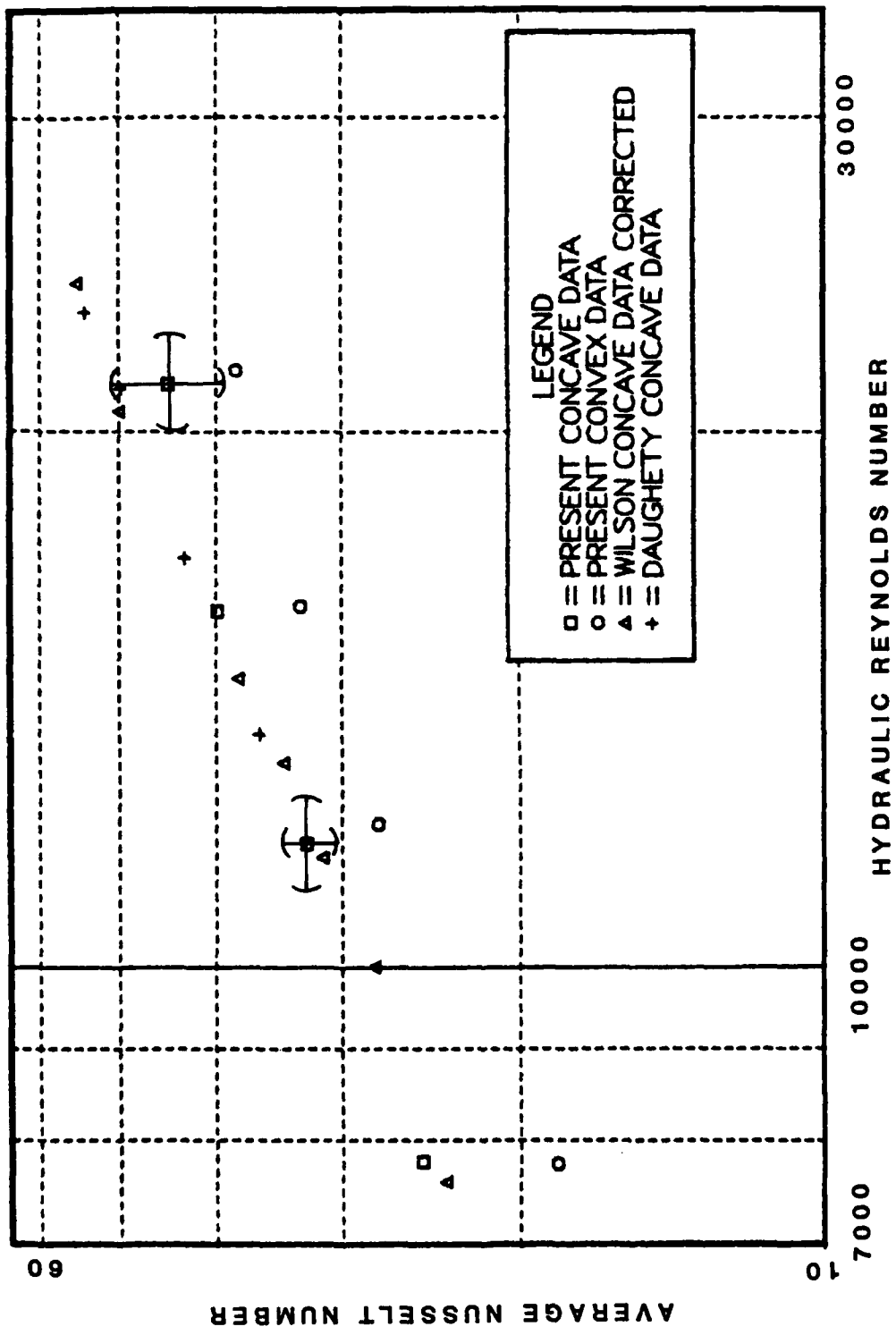


Figure 32. Comparison of Present Data with Daughety and Corrected Wilson, Curved Section.

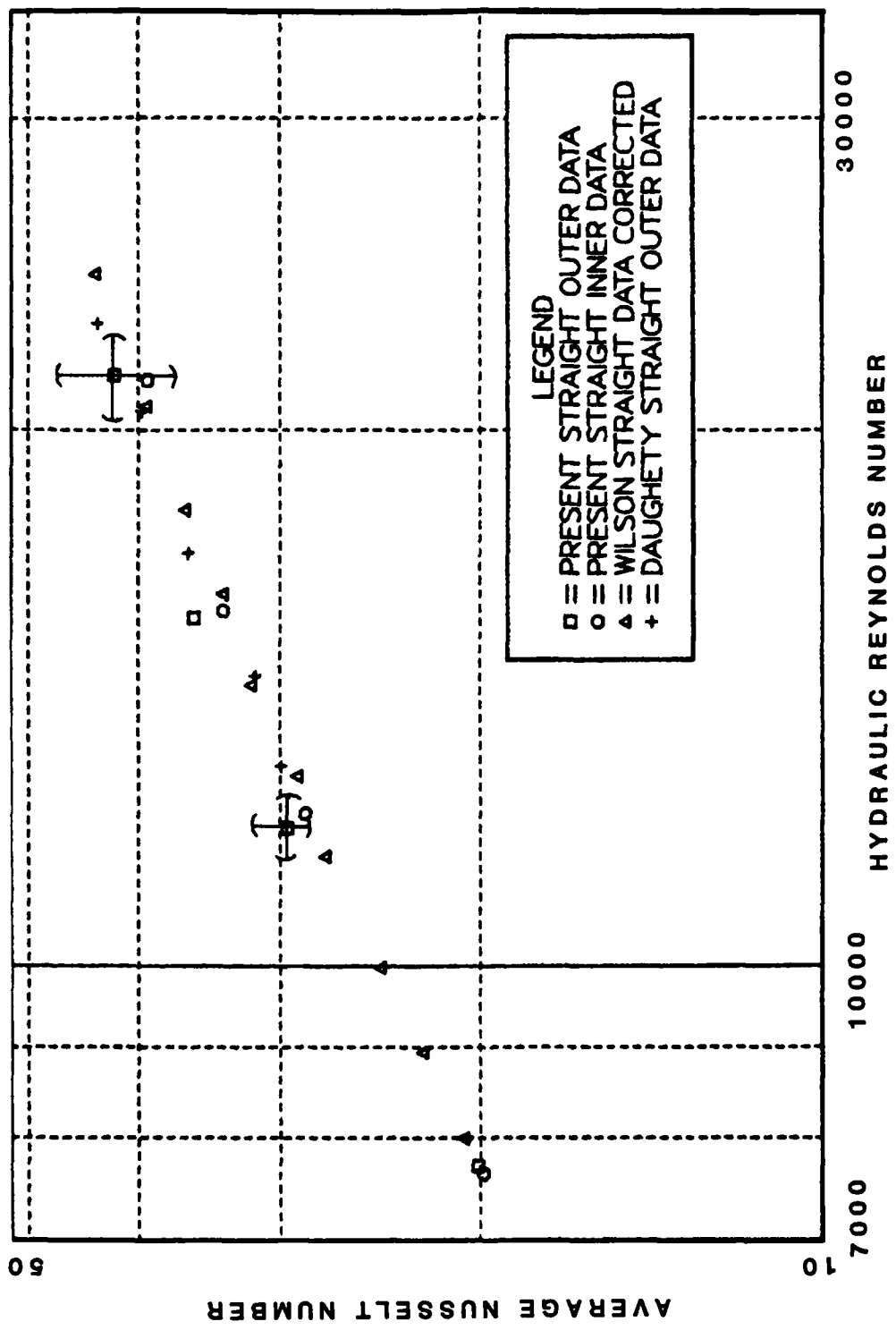


Figure 33. Comparison of Present Data with Daughety and Corrected Wilson, Straight Section.

and thirty percent for transition flows. Daughety [Ref. 27], reported an increase of twenty percent in the heat transfer rate for turbulent flows. Wilson [Ref. 28], reported an increase of forty-five percent for laminar flows, twenty percent for transition flows, thirteen percent for hydraulic Reynolds numbers between 5400 and 12000, and about twenty-six percent at a hydraulic Reynolds number of 24000. This compares very favorably with the present results, except for the data at a hydraulic Reynolds number of 21000. No conclusion can be made about the present results at a hydraulic Reynolds number of 21000 because of the high uncertainty of the data as previously mentioned. This area needs further experimentation before accurate conclusions can be made about the heat transfer rate at high hydraulic Reynolds numbers.

Kreith [Ref. 16] reported an increase in the rate of heat transfer along a concave wall as compared to a convex wall of twenty-five to sixty percent for hydraulic Reynolds numbers between 10^4 to 10^6 . This also compares favorably with the present results which indicate an increase of seventeen to thirty-eight percent when comparing concave wall to convex wall.

A comparison of analytical and experimental results with those of the present study for the straight test section is shown graphically in Figure 34. The Dittus-Boelter equation

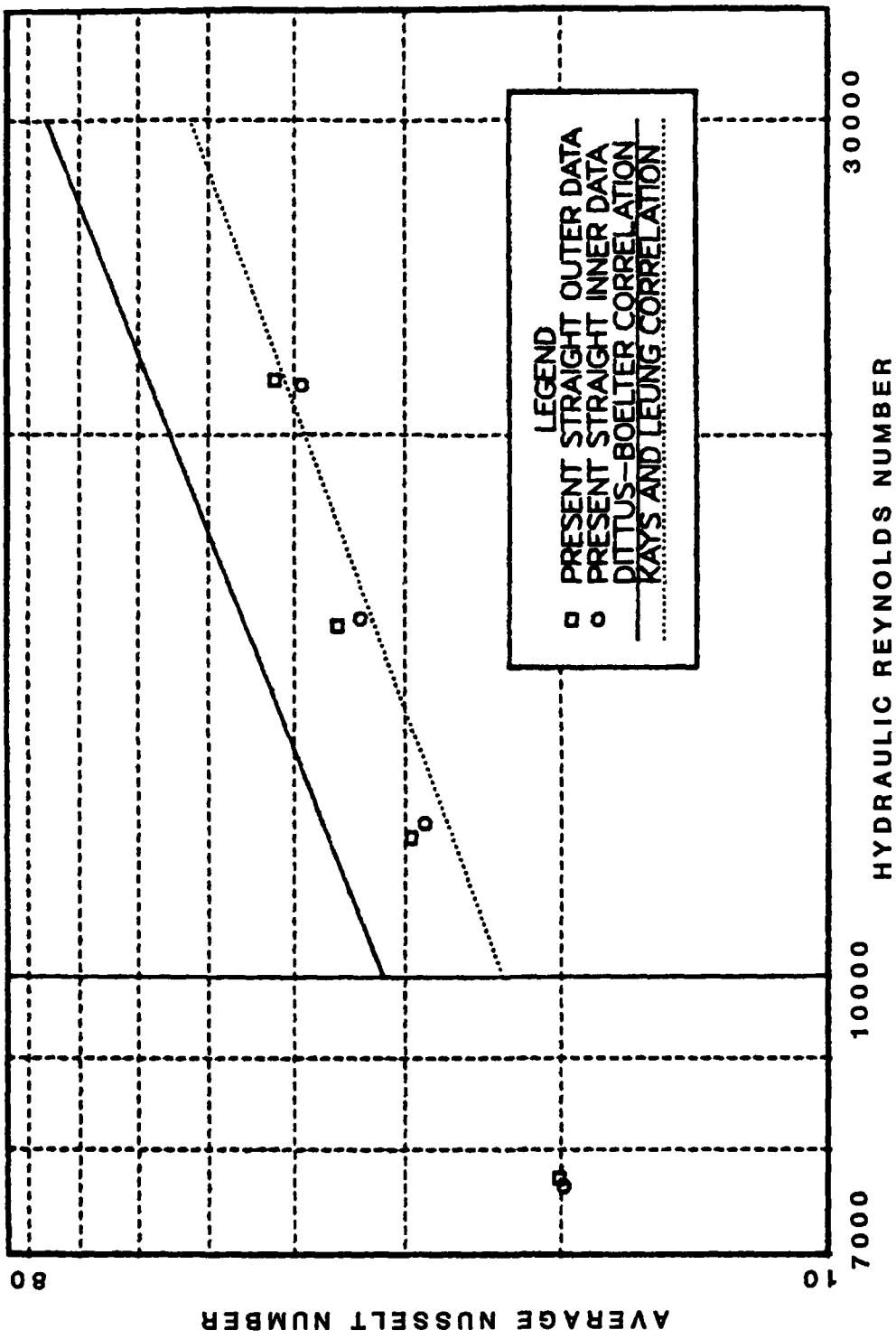


Figure 34. Comparison of Present Data with Dittus-Boelter, Kays and Leung, for Turbulent Flow, Straight Section.

[Ref. 29] for heat transfer in a straight tube for constant wall temperature is plotted from:

$$Nu = 0.02Re^{0.8}$$

For a Prandtl number equal to 0.71. Additionally, the results of Kays and Leung [Ref. 21] for heat transfer in annular passages are shown for $r^* = 1.0$, which equates to parallel plates. When examined these results compare favorably with the present data.

The curved section data is plotted in Figure 35, and is compared to the experimental work of Brinich and Graham [Ref. 22]. The accuracy of the data points used from Brinich and Graham are subject to some error, in that the actual values are not given in their study and had to be taken from a plot of Stanton number versus Reynolds number.

After carefully examining the past and present data the trends and results are consistent. Heat transfer rates increase with increasing Reynolds numbers. Also, the concave curved section enhances the rate of heat transfer over the convex curved section and the straight test sections for laminar, transition, and turbulent flows. The presence of Taylor-Gortler vortices in the laminar and transition regime seems to be the major contributing factor to this enhancement. Whether the Taylor-Gortler vortices continue to exist in the turbulent flow regime remains to be seen.

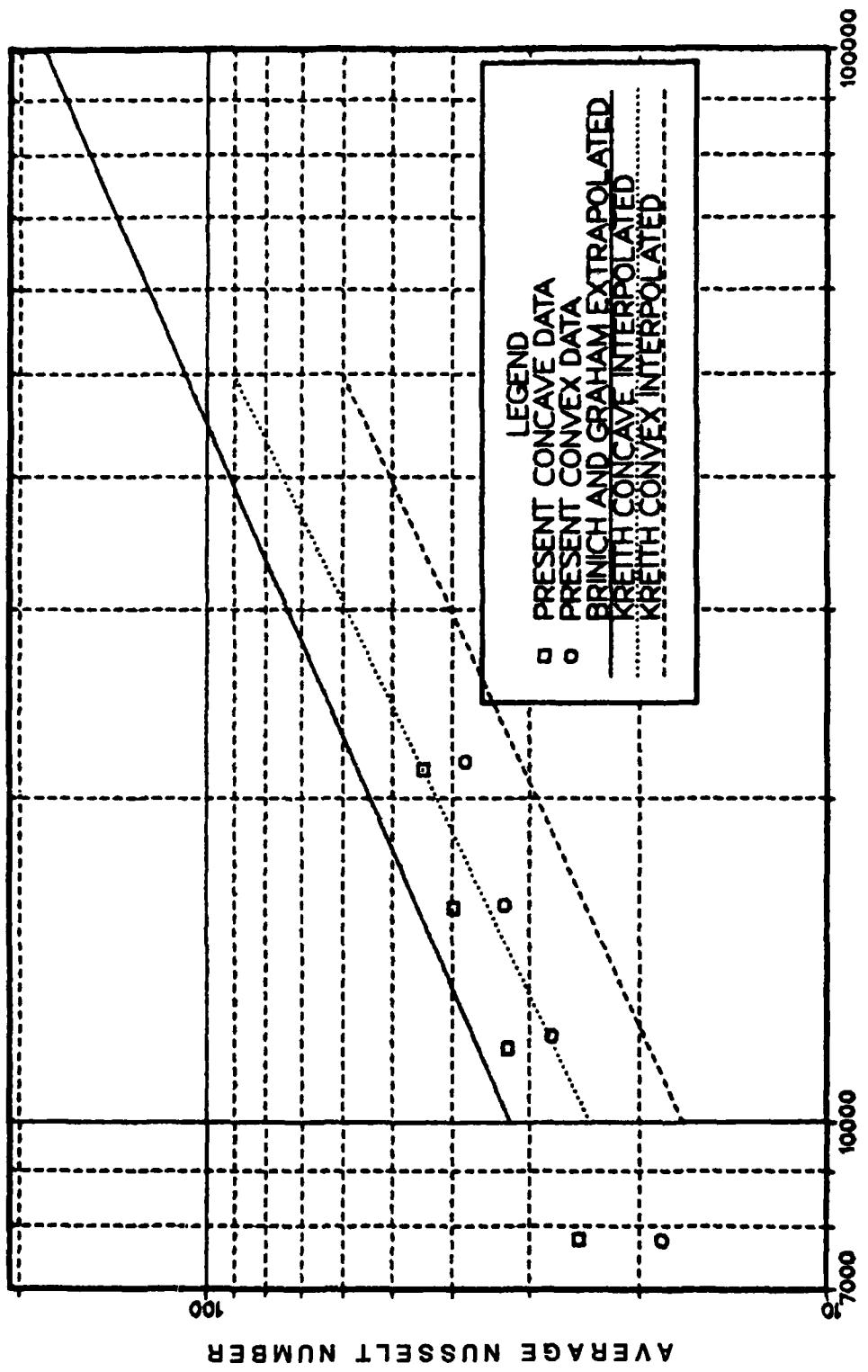


Figure 35. Comparison of Present Data with Brinich and Graham, and Kreith, for Turbulent Flow, Curved Section.

VII. RECOMMENDATIONS

The amount of experimental work remaining in the study of heat transfer in curved channels is still significant. The present experimental apparatus has been tested in the turbulent regime, and the test data proves that accurate results can be obtained for hydraulic Reynolds numbers below 17000, slightly higher when heating the straight test section. Additional experiments into the laminar, transition, and turbulent region should be conducted to better understand the heat transfer processes occurring in the straight and curved sections. By remaining below a hydraulic Reynolds number of 17000 accurate data can be obtained and significant conclusions can be drawn in the comparison of the curved sections to the straight section, and the concave curved wall to the convex curved wall.

To improve the accuracy of the data and results some slight modifications to the present channel should be done. First, the straight outlet section of the channel should be lengthened to ensure proper mixing of the heated outlet air. Second, some sort of honey combing, screening, or other type of device should be placed in the outlet section to enhance the mixing of the heated outlet air. Finally, extra thermocouples should be placed at the outlet and read more

then once during a data run to decrease the uncertainty of the outlet air temperature (T_{out}) and the uncertainty of the difference between the inlet and outlet air temperature. By applying these recommendations the uncertainty of the Nusselt number can be reduced to four percent or less.

Further experiments at hydraulic Reynolds numbers greater than 17000 also need to be examined. This can be accomplished if the above recommendations are taken along with one other. The channel walls need outer support to prevent the center of the channel from collapsing at the high hydraulic Reynolds numbers. Slight collapsing was noticed at hydraulic Reynolds numbers greater than 20000. This collapsing was caused by the laminating of two 0.3175 centimeter thick walls which were not as rigid as the single 0.635 centimeter thick walls used previously. The actual hydraulic Reynolds numbers that can be attained and still yield accurate results will be limited by the power of the compressor and the rigidity of the channel's walls.

Finally, once a strong data base can be obtained for each test section further experimentation can be conducted with different boundary conditions. For example, both curved walls heated at the same constant heat flux. Once this can be done a true comparison of the heat transfer rate of the total curved test section can be compared to the total straight test section, i.e., both curved walls versus both straight walls.

APPENDIX A: COMPUTER PROGRAM

```
1000 ! FILE NAME: DRP2A
1010 ! LAST REVISION DATE: 21 OCTOBER 1985
1020 ! AUTHOR: LT. GEORGE G. GALYO
1030!
1040 ! PROGRAM FOR GATHERING AND REDUCING DATA WHEN HEATING ONE COPPER PLATE,
1050 ! WITH 10 MINUTES BETWEEN RUNS. PROGRAM IS MODIFIED TO ACCOUNT FOR
1060 ! BROKEN THERMOCOUPLE CHANNELS 5, 16, 21, AND 26 WHICH EFFECT OUTER
1070 ! CURVED HEATER, AND THERMOCOUPLE CHANNEL 47 WHICH EFFECTS INNER CURVED
1080 ! HEATER.
1090!
1100 COM /Co/ D(7),Aa(76,2)
1110 DIM Emf(79),T(79)
1120!
1130 ! CORRELATION FACTORS FOR EMF TO DEGREES CELSIUS FOR CU-CO T/C.
1140!
1150 DATA 0.10086091,25727.94369,-767345.8295,78025595.81
1160 DATA -9247486589,6.97688E+11,-2.66192E+13,3.94078E+14
1170 READ D(*)
1180 PRINTER IS 701
1190 BEEP
1200 INPUT "ENTER MONTH, DAY, AND TIME (MM:DD:HH:MM:SS)",Time$
1210 OUTPUT 709;"TD";Time$
1220 BEEP
1230 INPUT "ENTER INPUT MODE (0=3054A,1=FILE)",Im
1240 IF Im=1 THEN
1250 BEEP
1260 INPUT "ENTER NAME OF EXISTING DATA FILE",Oldfile$
1270 PRINT USING "20X,""These Results Are From Data File: "",10A";Oldfile$
1280 PRINT
1290 PRINT
1300 ELSE
1310 BEEP
1320 INPUT "ENTER NAME OF NEW DATA FILE?",Newfile$
1330 PRINT USING "20X,""Data For This Run Is Stored In Data File: "",10A";Newf
ile$
1340 PRINT
1350 PRINT
1360 END IF
1370!
1380 ! ENTER THE CHANNEL CONFIGURATION.
1390!
1400 PRINT USING "9X,""THE FOLLOWING CHANNEL CONFIGURATION WAS SELECTED:"""
1410 PRINT
1420 BEEP
1430 INPUT "SELECT HEATER TYPE (0=STRAIGHT, 1=CURVED)",Itype
1440 IF Itype=0 THEN PRINT USING "12X,""Heating STRAIGHT Test Section."""
1450 IF Itype=1 THEN PRINT USING "12X,""Heating CURVED Test Section."""
1460 BEEP
1470 INPUT "SELECT HEATER POSITION (0=OUTER, 1=INNER)",Ipos
1480 IF Ipos=0 THEN PRINT USING "12X,""Heating OUTER Plate."""
1490 IF Ipos=1 THEN PRINT USING "12X,""Heating INNER Plate."""
1500 PRINT
1510!
1520 ! ENTERS FILES WITH T/C CALIBRATION COEFFICIENTS BASED ON HEATER TYPE.
1530!
1540 IF Itype=0 THEN ASSIGN @Filec TO "STRA_COEF"
1550 IF Itype=1 THEN ASSIGN @Filec TO "CURV_COEF"
1560 FOR I=0 TO 76
1570 ENTER @Filec:Aa(I,0),Aa(I,1),Aa(I,2)
1580 NEXT I
```

```

1590 ASSIGN @Filec TO *
1600! ! INSERT DATA STORAGE DISK.
1620!
1630 BEEP
1640 INPUT "CHANGE DISK AND HIT ENTER";Ok
1650 IF Im=1 THEN ASSIGN @File TO Oldfile$ 
1660 IF Im=0 THEN
1670 CREATE BDAT Newfile$,40
1680 ASSIGN @File TO Newfile$ 
1690 END IF
1700 ENTER 709;Time$ 
1710 CLEAR 709
1720 PRINT USING "20X, ""Month, Day, and Time: "" .14A";Time$ 
1730 PRINT
1740!
1750 ! FOR DATA RUN READ AND STORE ALL RAW EMF VALUES.
1760!
1770 IF Im=0 THEN
1780 OUTPUT 709;"AR AF00 AL79"
1790 OUTPUT 722;"F1 R1 T1 Z1 FL1"
1800 FOR I=0 TO 79
1810 OUTPUT 709;"AS"
1820 ENTER 722;Emf(I)
1830 NEXT I
1840 OUTPUT @File;Emf(*)
1850 ELSE
1860 ENTER @File;Emf(*)
1870 END IF
1880 OUTPUT 709;"TD"
1890!
1900 ! CONVERT AND CALIBRATE ALL T/C READINGS TO DEGREES CELSIUS.
1910!
1920 PRINT USING "9X, ""THE FOLLOWING DATA WERE RECORDED: """
1930 PRINT
1940 FOR I=0 TO 79
1950 IF I=38 OR I=39 OR I=77 OR I=78 THEN
1960 IF (Ipos=0 AND I=38) OR (Ipos=1 AND I=77) THEN
1970 Iadd=0
1980 IF Ipos=1 THEN Iadd=39
1990 PRINT USING "12X, ""Heater Voltage (Vh)      - "",2D.3D,"" (V)""";Emf(38+Ia
dd)
2000 PRINT USING "12X, ""Resistor Voltage (Vr)      - "",2D.3D,"" (V)""";Emf(39+Ia
dd)
2010 IF Ipos=0 THEN PRINT USING "12X, ""Precision Resistor (Rpr) = 2.01729 (Ohm
s)"""
2020 IF Ipos=1 THEN PRINT USING "12X, ""Precision Resistor (Rpr) = 2.00839 (Ohm
s)"""
2030 PRINT
2040 END IF
2050 ELSE
2060!
2070 ! IF T/C OUT OF RANGE PRINT A QUE.
2080!
2090 Aemf=Emf(I)
2100 IF Aemf<3.E-4 OR Aemf>3.E-3 THEN
2110 T(I)=999.99
2120 ELSE
2130 CALL Tvsy(Emf(I),Tt)
2140 IF I=79 THEN

```

```

2150 T(I)=Tt
2160 GOTO 2210
2170 END IF
2180 T(I)=FNTcorr(Tt,I)
2190 END IF
2200 END IF
2210 NEXT I
2220!
2230 ! PRINT ALL T/C READINGS.
2240!
2250 PRINT USING "12X, ""OUTER PLATE: """
2260 PRINT USING "14X, ""T/C Number:    1      2      3      4      5
6"""
2270 PRINT USING "14X, ""Temp (C):    "",6(3D.DD,2X)";T(0),T(1),T(2),T(3),T(4),T
(5)
2280 PRINT USING "14X, ""T/C Number:    7      8      9      10     11
12"""
2290 PRINT USING "14X, ""Temp (C):    "",6(3D.DD,2X)";T(6),T(7),T(8),T(9),T(10),
T(11)
2300 PRINT USING "14X, ""T/C Number:    13     14     15     16     17
18"""
2310 PRINT USING "14X, ""Temp (C):    "",6(3D.DD,2X)";T(12),T(13),T(14),T(15),T
(16),T(17)
2320 PRINT USING "14X, ""T/C Number:    19     20     21     22     23
24"""
2330 PRINT USING "14X, ""Temp (C):    "",6(3D.DD,2X)";T(18),T(19),T(20),T(21),T
(22),T(23)
2340 PRINT USING "14X, ""T/C Number:    25     26     27     28     29
30"""
2350 PRINT USING "14X, ""Temp (C):    "",6(3D.DD,2X)";T(24),T(25),T(26),T(27),T
(28),T(29)
2360 PRINT
2370!
2380 ! CALCULATE AVERAGE TEMPERATURE OF OUTER HEATED WALL.
2390!
2400 Sum=0.
2410 IF Itype=0 THEN
2420 FOR I=0 TO 29
2430 Sum=Sum+T(I)
2440 NEXT I
2450 Two=Sum/30
2460!
2470 ! CORRECTION FOR BROKEN T/C CHANNELS 5, 16, 21, AND 26 IN OUTER CURVED HE
ATER.
2480!
2490 ELSE
2500 FOR I=0 TO 29
2510 IF I=5 OR I=16 OR I=21 OR I=26 THEN 2530
2520 Sum=Sum+T(I)
2530 NEXT I
2540 Two=Sum/26
2550 END IF
2560 PRINT USING "12X, ""OUTER INSULATION: """
2570 PRINT USING "14X, ""T/C Number:    31 (Tins01)   32 (Tins02)   33 (Tins03)"
"""
2580 PRINT USING "14X, ""Temp (C):    "",3(3D.DD,8X)";T(30),T(31),T(32)
2590 Tins01=T(30)
2600 Tins02=T(31)
2610 Tins03=T(32)
2620 PRINT

```

```

2630 PRINT USING "12X,,"ORIFICE TEMP (Torf) = "",3D.DD,," (C)";T(33)
2640 PRINT
2650 PRINT USING "12X,,"INLET TEMPERATURE:"""
2660 PRINT USING "14X,,"T/C Number:    35      36      37      38"""
2670 PRINT USING "14X,,"Temp (C):    "",4(3D.DD,2X);T(34),T(35),T(36),T(37)
2680 PRINT
2690!
2700 ! CALCULATE AVERAGE INLET TEMPERATURE.
2710!
2720 Sum=0.
2730 FOR I=34 TO 37
2740 Sum=Sum+T(I)
2750 NEXT I
2760 Tin=Sum/4
2770 PRINT USING "12X,,"INNER PLATE:"""
2780 PRINT USING "14X,,"T/C Number:    41      42      43      44      45
46"""
2790 PRINT USING "14X,,"Temp (C):    "",6(3D.DD,2X);T(40),T(41),T(42),T(43),T(
44),T(45)
2800 PRINT USING "14X,,"T/C Number:    47      48      49      50      51
52"""
2810 PRINT USING "14X,,"Temp (C):    "",6(3D.DD,2X);T(46),T(47),T(48),T(49),T(
50),T(51)
2820 PRINT USING "14X,,"T/C Number:    53      54      55      56      57
58"""
2830 PRINT USING "14X,,"Temp (C):    "",6(3D.DD,2X);T(52),T(53),T(54),T(55),T(
56),T(57)
2840 PRINT USING "14X,,"T/C Number:    59      60      61      62      63
64"""
2850 PRINT USING "14X,,"Temp (C):    "",6(3D.DD,2X);T(58),T(59),T(60),T(61),T(
62),T(63)
2860 PRINT USING "14X,,"T/C Number:    65      66      67      68      69
70"""
2870 PRINT USING "14X,,"Temp (C):    "",6(3D.DD,2X);T(64),T(65),T(66),T(67),T(
68),T(69)
2880 PRINT
2890!
2900 ! CALCULATE AVERAGE TEMPERATURE OF INNER HEATED WALL.
2910!
2920 Sum=0.
2930 IF Itype=0 THEN
2940 FOR I=40 TO 69
2950 Sum=Sum+T(I)
2960 NEXT I
2970 Twi=Sum/30
2980!
2990 ! CORRECTION FOR BROKEN T/C CHANNEL 47 IN INNER CURVED HEATER.
3000!
3010 ELSE
3020 FOR I=40 TO 69
3030 IF I=47 THEN 3050
3040 Sum=Sum+T(I)
3050 NEXT I
3060 Twi=Sum/29
3070 END IF
3080 PRINT USING "12X,,"INNER INSULATION:"""
3090 PRINT USING "14X,,"T/C Number:    71 (Tinsi1)  72 (Tinsi2)  73 (Tinsi3)
3100 PRINT USING "14X,,"Temp (C):    "",3(3D.DD,8X);T(70),T(71),T(72)
3110 Tinsi1=T(70)

```

```

3120 Tinsi2=T(71)
3130 Tinsi3=T(72)
3140 PRINT
3150 PRINT USING "12X,OUTLET TEMPERATURE:***"
3160 PRINT USING "14X,T/C Number:    74      75      76      77***"
3170 PRINT USING "14X,Temp (C):    .4(3D.DD.2X)*;T(73),T(74),T(75),T(76)"
3180 PRINT USING "@,*"
3190!
3200 ! CALCULATE AVERAGE OUTLET TEMPERATURE.
3210!
3220 Sum=0.
3230 FOR I=73 TO 76
3240 Sum=Sum+T(I)
3250 NEXT I
3260 Tout=Sum/4
3270!
3280 ! CALCULATE DIFFERENCE BETWEEN CHANNEL INLET AND OUTLET TEMPERATURES.
3290!
3300 Tdiff=Tout-Tin
3310!
3320 ! CALCULATE CHANNEL BULK TEMPERATURE.
3330!
3340 Tblk=(Tin+Tout)/2
3350!
3360 ! PRINT CALCULATED TEMPERATURES.
3370!
3380 PRINT USING "9X,THE FOLLOWING TEMPERATURES WERE CALCULATED:***"
3390 PRINT
3400 PRINT USING "12X,Average Outer Wall Temperature (Two)      - **,3D."
DD,-- (C)***;Two
3410 PRINT USING "12X,Average Inner Wall Temperature (Twi)      - **,3D."
DD,-- (C)***;Twi
3420 PRINT USING "12X,Average Outlet Temperature (Tout)      - **,3D."
DD,-- (C)***;Tout
3430 PRINT USING "12X,Average Inlet Temperature (Tin)      - **,3D."
DD,-- (C)***;Tin
3440 PRINT USING "12X,Channel Inlet and Outlet Temp Diff (Tdiff)      - **,3D."
DD,-- (C)***;Tdiff
3450 PRINT USING "12X,Average Bulk Temperature (Tblk)      - **,3D."
DD,-- (C)***;Tblk
3460!
3470 ! CALCULATE DELTA T (Tdel) FOR USE IN CALCULATING H LATER.
3480!
3490 Tdelo=Two-Tblk
3500 Tdeli=Twi-Tblk
3510 IF Ipos=0 THEN Tdel=Tdelo
3520 IF Ipos=1 THEN Tdel=Tdeli
3530 PRINT USING "12X,Mean Temperature Difference (Tdel)      - **,3D."
DD,-- (C)***;Tdel
3540!
3550 ! CALCULATE DIFFERENCE BETWEEN OUTER AND INNER WALL.
3560!
3570 Twdiff=ABS(Two-Twi)
3580 PRINT USING "12X,Outer and Inner Wall Temp Difference (Twdiff)      - **,3D."
DD,-- (C)***;Twdiff
3590!
3600 ! CALCULATE LOCAL CHANNEL TEMPERATURES AT INLET, MIDDLE AND OUTLET.
3610!
3620 Tin=Tin+(.5*Tdiff/12)
3630 Tcmid=Tin+(4.5*Tdiff/12)

```

```

3640 Tcout=Tin+(11.5*Tdiff/12)
3650 PRINT USING "12X,,"Average Local Channel Temp at Inlet (Tcin) - "",3D.
DD,-- (C)"";Tcin
3660 PRINT USING "12X,,"Average Local Channel Temp at Middle (Tcmid) - "",3D.
DD,-- (C)"";Tcmid
3670 PRINT USING "12X,,"Average Local Channel Temp at Outlet (Tcout) - "",3D.
DD,-- (C)"";Tcout
3680!
3690 ! CALCULATE AVERAGE LOCAL HEATED WALL TEMPERATURE AT INLET.
3700!
3710 Sum=0.
3720 Iadd=0
3730 IF Ipos=1 THEN Iadd=40
3740!
3750 ! CORRECTION FOR BROKEN T/C CHANNELS 5, AND 47 CURVED HEATER ONLY.
3760!
3770 IF Itype=1 THEN
3780 FOR I=0 TO 6
3790 IF (Ipos=0 AND I=5) OR (Ipos=1 AND I=6) THEN 3810
3800 Sum=Sum+T(I+Iadd)
3810 NEXT I
3820 Twin=Sum/6
3830 ELSE
3840 FOR I=0 TO 7
3850 IF (Ipos=0 AND I=7) OR (Ipos=1 AND I=6) THEN 3870
3860 Sum=Sum+T(I+Iadd)
3870 NEXT I
3880 Twin=Sum/7
3890 END IF
3900 PRINT USING "12X,,"Avg Local Heated Wall Temp at Inlet (Twin) - "",3D.
DD,-- (C)"";Twin
3910!
3920 ! CALCULATE AVERAGE LOCAL HEATED WALL TEMPERATURE NEAR MIDDLE.
3930!
3940 Sum=0.
3950!
3960 ! CORRECTION FOR BROKEN T/C CHANNEL 16 CURVED HEATER ONLY.
3970!
3980 IF Itype=1 AND Ipos=0 THEN
3990 FOR I=9 TO 15
4000 IF I=10 THEN 4020
4010 Sum=Sum+T(I)
4020 NEXT I
4030 Twmid=Sum/6
4040 ELSE
4050 FOR I=9 TO 16
4060 IF (Ipos=0 AND I=10) OR (Ipos=1 AND I=9) THEN 4080
4070 Sum=Sum+T(I+Iadd)
4080 NEXT I
4090 Twmid=Sum/7
4100 END IF
4110 PRINT USING "12X,,"Avg Local Heated Wall Temp Near Middle (Twmid) - "",3D.
DD,-- (C)"";Twmid
4120!
4130 ! CALCULATE AVERAGE LOCAL HEATED WALL TEMPERATURE AT OUTLET.
4140!
4150 Sum=0.
4160!
4170 ! CORRECTION FOR BROKEN T/C CHANNEL 26 CURVED HEATER ONLY.
4180!

```

```

4190 IF Itype=1 AND Ipos=0 THEN
4200 FOR I=23 TO 29
4210 IF I=26 THEN 4230
4220 Sum=Sum+T(I)
4230 NEXT I
4240 Twout=Sum/6
4250 ELSE
4260 FOR I=23 TO 29
4270 Sum=Sum+T(I+Iadd)
4280 NEXT I
4290 Twout=Sum/7
4300 END IF
4310 PRINT USING "12X,,"Avg Local Heated Wall Temp at Outlet (Twout) = "",3D.
4320 DD." (C)";Twout
4320 PRINT
4330 PRINT
4340!
4350 ! ENTER ORIFICE PRESSURE DATA.
4360!
4370 BEEP
4380 INPUT "ENTER PAtm (inHg), DPM(inH20), P1M(inH20), RE1",Patm,Dpm,P1m,Re1
4390 PRINT USING "9X,,"THE FOLLOWING ORIFICE DATA WERE ENTERED:"""
4400 PRINT
4410 PRINT USING "12X,,"Patm(inHg) DPM(inH20) P1M(inH20) RE1"""
4420 PRINT USING "14X,2(2D,DD,10X),(2D,DD,7X),5D,D";Patm,Dpm,P1m,Re1
4430 PRINT
4440!
4450 ! CONVERT PRESSURE READINGS TO SI UNITS AND P1M TO ABSOLUTE.
4460!
4470 Patm=Patm*3376.8
4480 Pdpm=Dpm*248.84
4490 P1=Ptm-(P1m*248.84)
4500 Torf=T(33)
4510!
4520 ! PHYSICAL PROPERTIES AND CONSTANTS.
4530!
4540 R=286.987 !FOR AIR.
4550 Rho=P1/(R*(Torf+273.15)) !DENSITY OF AIR AT ORIF PLATE.
4560 Gamma=1.40 !FOR AIR.
4570 Cp=1006 !Cp GOOD FOR Tblk BETWEEN 12 AND 33 (DEG C).
4580 Gc=1.0
4590 Sigma=5.669E-8
4600 Ecu=.12 !EMISSIVITY OF COPPER.
4610!
4620 ! DIMENSIONS OF CHANNEL.
4630!
4640 Dc=.006350
4650 Wid=.2540
4660 Ri=.297
4670 Pwet=2*(Dc+Wid)
4680 Ac=Dc*Wid
4690 Dhd=4*Ac/Pwet
4700 Apl=.0774192
4710!
4720 ! PROPERTIES OF INSULATION.
4730!
4740 Xins=.0127
4750 Kins=3.8E-2
4760!
4770 ! ENTER ORIFICE CONFIGURATION.

```

```

4780!
4790 BEEP
4800 INPUT "SELECT DIAMETER OF ORIFICE (0=.5334, 1=1.0755 (inches))",Size
4810 IF Size=0 THEN Dorf=.013548
4820 IF Size=1 THEN Dorf=.027318
4830!
4840 ! DIMENSIONS OF PIPE AND ORIFICE PLATE.
4850!
4860 A=(PI*Dorf^2)/4
4870 Dpipe=.051772
4880 Apipe=PI*Dpipe^2/4
4890 Beta=Dorf/Dpipe
4900 PRINT USING "12X,""Dorf(m)           A(m^2)          Beta"""
4910 PRINT USING "12X,(Z.6D,6X),(Z.3DE,6X),Z.4D";Dorf,A,Beta
4920 PRINT
4930 PRINT
4940!
4950 ! CORRELATION FOR EXPANSION FACTOR BASED ON 1D AND 1/2D TAPS.
4960!
4970 Y=1-(.41+.35*Beta^4)*(Pdel/(Gamma*P1))
4980!
4990 ! CALCULATION OF FLOW COEFFICIENT (K) IN SI UNITS.
5000!
5010 B=.0002+2.794E-5/Dpipe+(.0038+1.016E-5/Dpipe)*(Beta^2+(16.5+1.968504E+2*Dp
ipe)*Beta^16)
5020!
5030 ! K1 AND K2 ARE DUMMY VARIABLES TO CALCULATE Ko.
5040!
5050 K1=.6014-5.3974064E-3/Dpipe^.25
5060 K2=(-.376+2.8971138E-2/Dpipe^.25)*(1.6129E-7/(Dpipe^2*Beta^2+6.35E-5*Dpipe)
+Beta^4+1.5*Beta^16)
5070 Ko=K1+K2
5080 K=Ko+1000*B/Re1^.5
5090!
5100 ! Mu CORRELATION GOOD FOR Torf BETWEEN 17 AND 41 DEGREES CELSIUS.
5110!
5120 Mu=4.6971429E-8*Torf+1.7194722E-5
5130!
5140 ! CALCULATE Mdot AND REpipe AND COMPARE TO PREDICTED RE1.
5150!
5160 Mdot=K*A*Y*(2*Gc*Rho*Pdel)^.5
5170 Repipe=(Mdot*Dpipe)/(Mu*Apipe)
5180 Diff=(ABS(Re1-Repipe)/Re1)*100
5190 Re1=Repipe
5200 IF Diff>.001 THEN 5080
5210 PRINT USING "9X,""THE FOLLOWING DATA WERE CALCULATED:"""
5220 PRINT
5230 PRINT USING "12X,""Orifice Expansion Factor (Y)      :   .,Z.4D,":Y
5240 PRINT USING "12X,""Orifice Flow Coefficient (K)      :   .,Z.4D,":K
5250 PRINT USING "12X,""Density Based on Torf (Rho)      :   .,Z.4D,"" (kg/m^
3)"";Rho
5260 PRINT USING "12X,""Viscosity Based on Torf (Mu)      :   .,Z.3DE,"" (kg/m.s)
5270!
5280 ! Mu CORRELATION GOOD FOR Tblk BETWEEN 17 AND 41 DEGREES CELSIUS.
5290!
5300 Mu=4.6971429E-8*Tblk+1.7194722E-5
5310 Red=(Mdot*Dc)/(Mu*Ac)
5320 Rehd=(Mdot*Dhd)/(Mu*Ac)
5330!

```

```

5340 ! CALCULATION OF POWER INTO HEATER PLATE.
5350!
5360 Iadd=0
5370 IF Ipos=1 THEN Iadd=39
5380 IF Ipos=0 THEN Rpr=2.01729
5390 IF Ipos=1 THEN Rpr=2.00839
5400 Qp=(Emf(38+Iadd)*Emf(39+Iadd))/Rpt
5410!
5420 ! CALCULATION OF HEAT INPUT TO AIR.
5430!
5440 Qair=Mdot*Cp*(Tout-Tin)
5450!
5460 ! CALCULATE LOCAL HEAT TRANSFER COEF. AND NUSSELT NUMBER.
5470!
5480 Kair=7.7257143E-5*Tcin+.024165836
5490 Hin=Qair/(Apl*(Twin-Tcin))
5500 Nuin=(Hin*Dhd)/Kair
5510 Kair=7.7257143E-5*Tcmid+.024165836
5520 Hmid=Qair/(Apl*(Twmid-Tcmid))
5530 Numid=(Hmid*Dhd)/Kair
5540 Kair=7.7257143E-5*Tcout+.024165836
5550 Hout=Qair/(Apl*(Twout-Tcout))
5560 Nuout=(Hout*Dhd)/Kair
5570!
5580 ! Kair CORRELATION GOOD FOR Tblk BETWEEN 17 AND 41 DEGREES CELSIUS.
5590!
5600 Kair=7.7257143E-5*Tblk+.024165836
5610!
5620 ! CALCULATE AVERAGE HEAT TRANSFER COEF. AND NUSSELT NUMBER.
5630!
5640 Havg=Qair/(Apl*Tdel)
5650 Nuavg=(Havg*Dhd)/Kair
5660!
5670 ! CALCULATE HEAT LOSSES.
5680!
5690 Qlo1=(Kins*Apl*(Tinso1-Tinso2))/Xins
5700 Qlo2=(Kins*Apl*(Tinso2-Tinso3))/Xins
5710 Qlo=(Qlo1+Qlo2)/2
5720 Qli1=(Kins*Apl*(Tinsi1-Tinsi2))/Xins
5730 Qli2=(Kins*Apl*(Tinsi2-Tinsi3))/Xins
5740 Qli=(Qli1+Qli2)/2
5750 Rr=2.0*((1-Ecu)/(Apl*Ecu))+(1.0/Apl)
5760 Qr=(Sigma*(ABS((Two+273.15)^4-(Tw1+273.15)^4)))/Rr
5770 Qdel=Qp-Qair-Qlo1-Qli1
5780!
5790 ! CALCULATE DEAN NUMBER.
5800!
5810 De=.5*Red*((Dc/2)/R1)^.5
5820 PRINT USING "12X, ""Viscosity Based on Tblk (Mu) - "", .2Z.3DE, "" (kg/m.s)
***;Mu
5830 PRINT USING "12X, ""Therm Cond Based on Tblk (Kair) - "", .Z.3DE, "" (W/m.K)"
***;Kair
5840 PRINT
5850 PRINT USING "12X, ""Patm - "", .6D.DD, "" (N/m^2)""";Patm
5860 PRINT USING "12X, ""Pdel - "", .4D.DD, "" (N/m^2)""";Pdel
5870 PRINT USING "12X, ""P1 - "", .6D.DD, "" (N/m^2)""";P1
5880 PRINT USING "12X, ""Mdot - "", .Z.4D, "" (kg/s)""";Mdot
5890 PRINT USING "12X, ""Repipe - "", .6D.D";Repipe
5900 PRINT USING "12X, ""Red - "", .6D.D";Red
5910 PRINT USING "12X, ""Rehd - "", .6D.D";Rehd

```

```

5920!
5930 ! ONLY PRINT DEAN NUMBER WHEN HEATING CURVED SECTION.
5940!
5950 IF Itype=1 THEN PRINT USING "12X,,"De      -   "",4D.D";De
5960 PRINT
5970 PRINT USING "12X,,"Qp      -   "",3D.3D," (Watts)",,7X,,"Qair      -   "",3D.3D," (W
atts)";Qp,Qair
5980 PRINT USING "12X,,"Qlo1      -   "",2D.3D," (Watts)",,7X,,"Qli1      -   "",2D.3D,"
(Watts)";Qlo1,Qli1
5990 PRINT USING "12X,,"Qlo2      -   "",2D.3D," (Watts)",,7X,,"Qli2      -   "",2D.3D,"
(Watts)";Qlo2,Qli2
6000 PRINT USING "12X,,"Qlo      -   "",2D.3D," (Watts)",,7X,,"Qli      -   "",2D.3D,"
(Watts)";Qlo,Qli
6010 PRINT USING "12X,,"Qr      -   "",2D.3D," (Watts)",,7X,,"Qdel      -   "",2D.3D,"
(Watts)";Qr,Qdel
6020 PRINT
6030 PRINT USING "12X,,"Hin      -   "",3D.DD," (W/m^2C)",,7X,,"Nuin      -   "",3D.DD,";H
in,Nuin
6040 PRINT USING "12X,,"Hmid      -   "",3D.DD," (W/m^2C)",,7X,,"Numid      -   "",3D.DD,";H
mid,Numid
6050 PRINT USING "12X,,"Hout      -   "",3D.DD," (W/m^2C)",,7X,,"Nuout      -   "",3D.DD,";H
out,Nuout
6060 PRINT USING "12X,,"Havg      -   "",3D.DD," (W/m^2C)",,7X,,"Nuavg      -   "",3D.DD,";H
avg,Nuavg
6070 PRINT
6080 PRINT
6090 BEEP
6100 INPUT "WILL THERE BE ANOTHER RUN? (1=Y,0=N)".Go_on
6110 IF Go_on<>0 THEN
6120 PRINT USING "@,."
6130 IF Im=0 THEN WAIT 600
6140 GOTO 1700
6150 END IF
6160 PRINT USING "8X,,"END OF RUN"""
6170 PRINT USING "@,."
6180 PRINTER IS 1
6190 ASSIGN @File TO *
6200 END
6210!
6220 ! CONVERTS EMF TO DEGREES CELSIUS.
6230!
6240 SUB TvsV(V,T)
6250 COM /Co/ D(7),Aa(76,2)
6260 Sum=0
6270 FOR I=0 TO 7
6280 Sum=Sum+D(I)*V^I
6290 NEXT I
6300 T=Sum
6310 SUBEND
6320!
6330 ! CALIBRATES T/C READINGS.
6340!
6350 DEF FNTcorr(T,I)
6360 COM /Co/ D(7),Aa(76,2)
6370 Tc=Aa(I,0)
6380 FOR J=1 TO 2
6390 Tc=Tc+Aa(I,J)*T^J
6400 NEXT J
6410 RETURN Tc
6420 FNEND

```

APPENDIX B: SAMPLE CALCULATIONS

Figure 36 below, shows the major heat transfer components for each of the test sections. The sample calculations that follow, demonstrate the methods used by the computer to calculate these components as well as the Reynolds number, average heat transfer coefficient, and average Nusselt number for each set of data. Part A of Appendix B contains a sample printout of a data run, followed by a summation of the data. The sample calculations are for the concave curved section, but those for the straight section are similar.

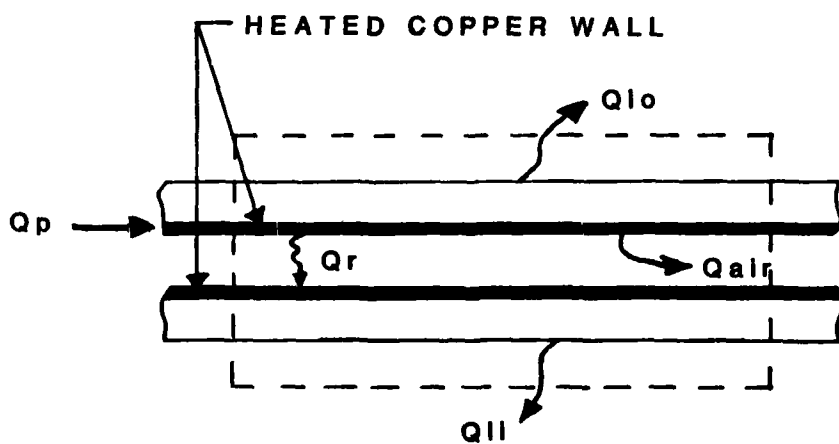


Figure 36. Energy Balance in Test Section.

1. SAMPLE CALCULATION DATA

THE FOLLOWING CHANNEL CONFIGURATION WAS SELECTED:

Heating CURVED Test Section.
Heating OUTER Plate.

Month, Day, and Time: 10:17:13:47:11

THE FOLLOWING DATA WERE RECORDED:

Heater Voltage (V_h) = 61.337 (V)
Resistor Voltage (V_r) = 5.195 (V)
Precision Resistor (R_{pr}) = 2.01729 (Ohms)

OUTER PLATE:

T/C Number:	1	2	3	4	5	6
Temp (C):	42.75	41.57	44.39	41.23	44.55	40.59
T/C Number:	7	8	9	10	11	12
Temp (C):	46.54	42.61	43.51	43.47	44.77	43.86
T/C Number:	13	14	15	16	17	18
Temp (C):	43.40	44.18	44.10	41.97	38.06	45.73
T/C Number:	19	20	21	22	23	24
Temp (C):	45.79	48.45	49.18	33.83	45.32	45.51
T/C Number:	25	26	27	28	29	30
Temp (C):	45.30	46.47	30.31	45.80	45.98	47.28

OUTER INSULATION:

T/C Number:	31 (T _{ins} o1)	32 (T _{ins} o2)	33 (T _{ins} o3)
Temp (C):	49.58	37.29	29.36

ORIFICE TEMP (T_{orf}) = 24.16 (C)

INLET TEMPERATURE:

T/C Number:	35	36	37	38
Temp (C):	20.55	20.48	20.47	20.43

INNER PLATE:

T/C Number:	41	42	43	44	45	46
Temp (C):	21.43	21.31	21.16	21.14	21.05	21.92
T/C Number:	47	48	49	50	51	52
Temp (C):	21.03	22.39	21.10	21.05	21.38	21.46
T/C Number:	53	54	55	56	57	58
Temp (C):	21.23	21.27	21.17	21.19	21.15	21.35
T/C Number:	59	60	61	62	63	64
Temp (C):	21.25	21.56	21.47	21.74	21.66	22.18
T/C Number:	65	66	67	68	69	70
Temp (C):	22.05	21.91	21.85	21.78	21.74	21.73

INNER INSULATION:

T/C Number:	71 (T _{ins} i1)	72 (T _{ins} i2)	73 (T _{ins} i3)
Temp (C):	21.53	21.49	21.32

OUTLET TEMPERATURE:

T/C Number:	74	75	76	77
Temp (C):	24.29	24.38	24.38	24.25

THE FOLLOWING TEMPERATURES WERE CALCULATED:

Average Outer Wall Temperature (Two)	=	44.76 (C)
Average Inner Wall Temperature (Twi)	=	21.46 (C)
Average Outlet Temperature (Tout)	=	24.32 (C)
Average Inlet Temperature (Tin)	=	20.48 (C)
Channel Inlet and Outlet Temp Diff (Tdiff)	=	3.84 (C)
Average Bulk Temperature (Tblk)	=	22.40 (C)
Mean Temperature Difference (Tdel)	=	22.36 (C)
Outer and Inner Wall Temp Difference (Twdiff)	=	23.30 (C)
Average Local Channel Temp at Inlet (Tcin)	=	20.64 (C)
Average Local Channel Temp at Middle (Tcmid)	=	21.92 (C)
Average Local Channel Temp at Outlet (Tcout)	=	24.16 (C)
Avg Local Heated Wall Temp at Inlet (Twin)	=	43.51 (C)
Avg Local Heated Wall Temp Near Middle (Twmid)	=	43.50 (C)
Avg Local Heated Wall Temp at Outlet (Twout)	=	46.06 (C)

THE FOLLOWING ORIFICE DATA WERE ENTERED:

Patm(inHg)	DPM(inH2O)	P1M(inH2O)	RE1
29.79	18.58	12.55	15500.0
Dorf(m)	A(m^2)	Beta	

THE FOLLOWING DATA WERE CALCULATED:

Orifice Expansion Factor (Y)	=	0.9852
Orifice Flow Coefficient (K)	=	0.6323
Density Based on Torf (Rho)	=	1.1424 (kg/m^3)
Viscosity Based on Torf (Mu)	=	18.330E-06 (kg/m.s)
Viscosity Based on Tblk (Mu)	=	18.247E-06 (kg/m.s)
Therm Cond Based on Tblk (Kair)	=	2.590E-02 (W/m.K)

Patm	=	100594.87 (N/m^2)	
Pdel	=	4623.45 (N/m^2)	
P1	=	97471.93 (N/m^2)	
Mdot	=	0.0375 (kg/s)	
Repipe	=	50352.2	
Red	=	8097.1	
Rehd	=	15799.1	
De	=	418.6	
Qp	=	157.971 (Watts)	Qair = 144.950 (Watts)
Qlo1	=	2.847 (Watts)	Qli1 = .009 (Watts)
Qlo2	=	1.838 (Watts)	Qli2 = .038 (Watts)
Qlo	=	2.342 (Watts)	Qli = .023 (Watts)
Qr	=	.751 (Watts)	Qdel = 9.415 (Watts)
Hin	=	81.90 (W/m^2C)	Nuin = 39.39
Hmid	=	86.78 (W/m^2C)	Numid = 41.58
Hout	=	85.51 (W/m^2C)	Nuout = 40.70
Havg	=	83.75 (W/m^2C)	Nuavg = 40.07

V_H	= 61.337 V
V_{PR}	= 5.195 V
R_{PR}	= 2.0173 Ω
P_{atm}	= 29.79 in. Hg
ΔP	= 18.58 in. H_2O
P_1	= 12.55 in. H_2O
T_{in}	= 20.48 C
T_{out}	= 24.32 C
T_{wo}	= 44.76 C
T_{wi}	= 21.49 C
$T_{ins,il}$	= 21.53 C
$T_{ins,i2}$	= 21.49 C
$T_{ins,01}$	= 49.58 C
$T_{ins,02}$	= 37.29 C
T_{orf}	= 24.16
K_{air}	= 25.90×10^{-3} W/mC
C_{pair}	= 1006 J/Kg K
μ_{air}	= $4.6971 \times 10^{-8} \times T_{air} + 1.71947 \times 10^{-5}$
K_{ins}	3.80×10^{-2} W/mC
ΔX_{ins}	= 0.0127 m
ϵ_{cu}	= 0.12
σ	= 5.669×10^{-8} W/m ² K ⁴
β	= .5277
γ	= 1.40
g_c	= 1 Kg m/Ns ²

$R = 286.98 \text{ Nm/Kg K}$
 $F_{wo-wi} = 1.0$
 $A_{PL} = .07742 \text{ m}^2$
 $A_c = .0016 \text{ m}^2$
 $A_{pipe} = .00211 \text{ m}^2$
 $D_c = .00635 \text{ m}$
 $D_{pipe} = .0518 \text{ m}$
 $D_{orf} = .027318 \text{ m}$
 $P_{wet} = .5207 \text{ m}$
 $R_i = .297 \text{ m}$

2. TEMPERATURE CALCULATIONS

a. Bulk Temperature (T_{blk})

$$T_{blk} = \frac{T_{in} + T_{out}}{2} = \frac{20.48 + 24.32}{2} = 22.40 \text{ C}$$

b. Mean Temperature Difference (ΔT)

$$\Delta T = T_{wo} - T_{blk} = 44.76 - 22.40 = 22.36$$

c. Temperature Difference Between Outer and Inner Wall (T_{wdiff})

$$T_{wdiff} = T_{wo} - T_{wi} = 44.76 - 21.49 = 23.27 \text{ C}$$

AD-R164 142

EXPERIMENTAL INVESTIGATION OF TURBULENT HEAT TRANSFER
IN STRAIGHT AND CURVED RECTANGULAR DUCTS(U) NAVAL
POSTGRADUATE SCHOOL MONTEREY CA G G GALYO DEC 85

2/2

UNCLASSIFIED

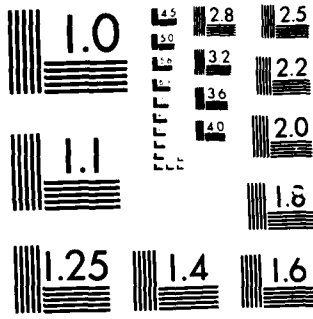
F/G 20/13

NL

[REDACTED]

END

FIGURE
LA
DPC



MICROCOPY RESOLUTION TEST CHART
NATIONAL BUREAU OF STANDARDS 1963 A

3. POWER CALCULATIONS

a. Power Supplied (Q_p)

$$Q_p = \frac{V_H V_{PR}}{R_{PR}} = \frac{(61.337)(5.195)}{(2.0173)} = 157.97 \text{ W}$$

b. Heat Lost Through the Back of the Outer Plate (Q_{lo})

$$Q_{lo} = \frac{T_{ins,o1} - T_{ins,o2}}{(\Delta X_{ins})/(K_{ins})(A_{PL})} = \frac{(49.58 - 37.29)}{(0.0127)/(3.80 \times 10^{-2})(.07742)} \\ = 2.85 \text{ W}$$

c. Heat Lost Through the Back of the Inner Plate (Q_i)

$$Q_{li} = \frac{T_{ins,i1} - T_{ins,i2}}{(\Delta X_{ins})/(K_{ins})(A_{PL})} = \frac{(21.53 - 21.49)}{(0.0127)/(3.80 \times 10^{-2})(.07742)} \\ = .01 \text{ W}$$

d. Heat Radiated (Q_r)

(1) Radiation Resistance (R_R)

$$R_R = 2 \times \left(\frac{1 - \epsilon_{cu}}{\frac{A_{PL}}{\epsilon_{cu}}} \right) + \frac{1}{A_{PL} F_{wo-wi}} \\ = \frac{1}{A_{PL}} \left[\frac{2}{\epsilon_{cu}} - 1 \right] = \frac{1}{0.07742} \left[\frac{2}{.12} - 1 \right] = 202.36 \text{ m}^{-2}$$

(2) Heat Radiated (Q_r)

$$Q_r = \frac{\sigma (T_{wo}^4 - T_{wi}^4)}{R_R} \quad T [=] K$$

$$= \frac{(5.669 \times 10^{-8}) [(44.76+273)^4 - (21.49+273)^4]}{202.36}$$
$$= 0.75 W$$

4. MASS FLOW RATE CALCULATIONS

a. Pressure Conversions

$$(1) P_{atm} = 29.79 \text{ in Hg} \times 3376.8 = 100594.87 \text{ N/m}^2$$

$$(2) \Delta P = 18.58 \text{ in H}_2\text{O} \times 248.84 = 4623.5 \text{ N/m}^2$$

$$(3) P_1 = (12.55 \text{ in H}_2\text{O} \times 248.84) - 100594.87$$
$$= 97471.93 \text{ N/m}^2$$

b. Density of Air (ρ_{air})

$$\rho_{air} = \frac{P_1}{R T_{or}} = \frac{(97471.93)}{(286.98)(24.16 + 273)} = 1.1424 \text{ Kg/m}^3$$

c. Expansion Factor (Y)

$$Y = 1 - [.41 + .35 \beta^4] \frac{\Delta P}{\gamma P_1}$$
$$= 1 - [.41 + .35 (.5277)^4] \frac{4623.5}{(1.40)(97471.93)}$$
$$= .9852$$

d. Area of Orifice (A)

$$A = \frac{\pi (D_{\text{orifice}})^2}{4} = \frac{\pi (.027318)^2}{4} = .005861 \text{ m}^2$$

e. Mass Flow Rate (\dot{m})

$$\dot{m} = YKA \quad 2g_c \rho_{\text{air}} \Delta P = (.9852)K(.0005861)$$

$$\times 2(1)(1.1424)(4623.5)$$

$$\dot{m} = .05935 \text{ K}$$

Iterating:

Assume a Pipe Reynolds number = 50000

Obtain a value for K, the flow coefficient, from
reference 30. K = .6325

Solve for \dot{m} . $\dot{m} = .0375 \text{ Kg/s}$

$$\text{Solve for new } Re_{\text{pipe}} = \frac{\dot{m} D_{\text{pipe}}}{A_{\text{pipe}} \mu_{\text{air}}} = \frac{(.0375)(.0518)}{(.00211)(18.33 \times 10^{-6})}$$

$$Re_{\text{pipe}} = 550225$$

Check convergence and repeat process if necessary.

(Convergence if difference less than .001)

$$\dot{m} = .0375 \text{ Kg/s}$$

5. REYNOLDS NUMBER CALCULATIONS

$$a. \quad Re_{\text{pipe}} = \frac{\dot{m} D_{\text{pipe}}}{A_{\text{pipe}} \mu_{\text{air}}} = \frac{(.0375)(.0518)}{(.00211)(18.33 \times 10^{-6})} = 50225$$

$$b. \quad Re_d = \frac{\dot{m} D_c}{A_c \mu_{\text{air}}} = \frac{(.0375)(.00635)}{(.0016)(18.25 \times 10^{-6})} = 8097.1$$

$$c. \quad Re_{\text{hd}} = \frac{\dot{m} D_{\text{hd}}}{A_c \mu_{\text{air}}}$$

$$(1) \quad D_{\text{hd}} = \frac{4 \times A_c}{P_{\text{wet}}} = \frac{(4)(.0016)}{.5207} = .01229 \text{ m}$$

$$Re_{\text{hd}} = \frac{\dot{m} D_{\text{hd}}}{A_c \mu_{\text{air}}} = \frac{(.0375)(.01229)}{(.0016)(18.25 \times 10^{-6})} = 15799.1$$

6. HEAT CONVECTED TO AIR CALCULATION

$$a. \quad Q_{\text{air}} = \dot{m} C_p (T_{\text{out}} - T_{\text{in}}) = (.0375)(1006)(24.32 - 20.48) = 144.95 \text{ W}$$

7. AVERAGE HEAT TRANSFER COEFFICIENT CALCULATION

$$\bar{h} = \frac{Q_{\text{air}}}{A_{\text{PL}} \Delta T} = \frac{144.95}{(.07742)(22.36)} = 83.72 \text{ W/m}^2\text{C}$$

8. AVERAGE NUSSELT NUMBER CALCULATION

$$\overline{Nu}_{\text{hd}} = \frac{\bar{h} D_{\text{hd}}}{k_{\text{air}}} = \frac{(83.73)(.01229)}{25.90 \times 10^{-3}} = 39.73$$

9. DEAN NUMBER CALCULATION

$$De = \frac{Re_d}{2} \sqrt{\frac{D_c/2}{R_l}} = \frac{8097.1}{2} \sqrt{\frac{.00635/2}{.297}} = 418.6$$

APPENDIX C: EXPERIMENTAL UNCERTAINTY

The uncertainties for the major variable in the experiments, were calculated in accordance with the method described by S. Kline and F. McClintoch [Ref. 33]. The estimates of the uncertainty in the measured quantities were made conservatively. As a result, there is considerable confidence in the uncertainties as calculated.

The following equations were used to calculate the uncertainties:

$$(1) \quad \frac{d\rho}{\rho} = \left(\left(\frac{dR}{R} \right)^2 + \left(\frac{dP_1}{P_1} \right)^2 + \left(\frac{dT_{orf}}{T_{orf}} \right)^2 \right)^{1/2}$$

$$(2) \quad \frac{\dot{dm}}{m} = \left[\left(\frac{dy}{y} \right)^2 + \left(\frac{dK}{K} \right)^2 + \left(\frac{dA}{A} \right)^2 \right]^{1/2} \\ + \left(1/4 \left(\left(\frac{dp_{air}}{p_{air}} \right)^2 + \left(\frac{d\Delta P}{\Delta P} \right)^2 \right) \right]$$

$$(3) \quad \frac{dQ_{air}}{Q_{air}} = \left(\left(\frac{\dot{dm}}{m} \right)^2 + \left(\frac{dC_{pair}}{C_{pair}} \right)^2 + \left(\frac{d(T_{out}-T_{in})}{T_{out}-T_{in}} \right)^2 \right)^{1/2}$$

$$(4) \quad \frac{\bar{h}}{h} = \left(\left(\frac{dQ_{air}}{Q_{air}} \right)^2 + \left(\frac{dA_{PL}}{A_{PL}} \right)^2 + \left(\frac{d\Delta T}{\Delta T} \right)^2 \right)^{1/2}$$

$$(5) \quad \frac{\bar{Nu}_{hd}}{Nu_{hd}} = \left(\left(\frac{\bar{h}}{h} \right)^2 + \left(\frac{dD_{hd}}{D_{hd}} \right)^2 + \left(\frac{dK_{air}}{K_{air}} \right)^2 \right)^{1/2}$$

$$(6) \frac{dRe_{hd}}{Re_{hd}} = \left(\left(\frac{dm}{m} \right)^2 + \left(\frac{dD_{hd}}{D_{hd}} \right)^2 + \left(\frac{du_{air}}{u_{air}} \right)^2 + \left(\frac{dA_c}{A_c} \right)^2 \right)^{1/2}$$

The following quantities had their uncertainty calculated by dividing the estimated error in the quantity by the value of the quantity, and these uncertainties are considered constant for the range of values in this experiment:

<u>Quantity</u>	<u>Uncertainty</u>
A	.0093
A_c	.0408
A_{PL}	.0080
c_{pair}	.0020
D _c	.0400
D _{hd}	.0396
K	.0030
K _{air}	.0038
P _{atm}	.0010
R	.0003
W _{id}	.0080
Y	.0020
u_{air}	.0054

The following quantities had the worst case error for hydraulic Reynolds numbers below 17000:

<u>Quantity</u>	<u>Error</u>
T_{blk}	$\pm .1^\circ C$
T_{in}	$\pm .1^\circ C$
T_{orf}	$\pm .1^\circ C$
T_{out}	$\pm .1^\circ C$
T_{wo}	$\pm .1^\circ C$
$T_{out} - T_{in}$	$\pm .2^\circ C$
ΔT	$\pm .2^\circ C$

For hydraulic Reynolds numbers greater than 17000 the error in the outlet temperature was much higher, as mentioned previously, and the following errors apply:

<u>Quantity</u>	<u>Error</u>
T_{blk}	$\pm .2^\circ C$
T_{in}	$\pm .1^\circ C$
T_{orf}	$\pm .1^\circ C$
T_{out}	$\pm .3^\circ C$
T_{wo}	$\pm .1^\circ C$
$T_{out} - T_{in}$	$\pm .4^\circ C$
ΔT	$\pm .3^\circ C$

The uncertainties for the following quantities were calculated using the sample data for the outer curved test section at a hydraulic Reynolds number of 15800:

<u>Quantity</u>	<u>Uncertainty</u>
P_1	.0159
ΔP	.0108
T_{orf}	.0003
$T_{out} - T_{in}$.0521
ΔT	.0089
ρ_{air}	.0159
\dot{m}	.0139
Q_{air}	.0540
h	.0553
Nu_{hd}	.0681
Re_{hd}	.0588

The uncertainty for the following quantities were calculated for the outer curved test section at a hydraulic Reynolds number of 21200:

<u>Quantity</u>	<u>Uncertainty</u>
P_1	.0043
ΔP	.0053
T_{orf}	.0003
$T_{out} - T_{in}$.1039
ΔT	.0111
ρ_{air}	.0043
\dot{m}	.0105
Q_{air}	.1044

\bar{h}	.1053
$\bar{N}_{u_{hd}}$.1126
$R_{e_{hd}}$.0581

By multiplying the quantity by its uncertainty the possible error can be calculated. The previous uncertainty calculations for a hydraulic Reynolds number of 15800 yielded $\bar{N}_{u_{hd}} = 40.07 \pm 2.73$ and a $R_{e_{hd}} = 15800 \pm 928$. For the run at a hydraulic Reynolds number of 21200 the $\bar{N}_{u_{hd}} = 44.71 \pm 5.03$ and a $R_{e_{hd}} = 21200 \pm 1232$.

The major source of uncertainty in the average Nusselt number is the uncertainty in the difference between the outlet and inlet air temperature. If this uncertainty can be brought below four percent, then the uncertainty of the average Nusselt number will be dictated by the uncertainty of the measured dimensions of the channel. In particular, the channel height (D_c) which has an uncertainty $dD_c/D_c = .0400$. The uncertainty of the channel height can only be reduced by increasing the channel height, and/or using materials with better tolerances.

LIST OF REFERENCES

1. Taylor, G. I., "Stability of a Viscous Liquid Contained Between Two Rotating Cylinders," Philosophical Transactions of the Royal Society of London, Series A, V. 233, pp. 289-343, 1923.
2. National Advisory Committee for Aeronautics, Technical Memorandum 1375, On the Three Dimensional Instability of Laminar Boundary Layers on Concave Walls, by H. Gortler, 1942.
3. Smith, A. M. O., "On the Growth of Taylor-Gortler Vortices Along Highly Concave Walls," Quarterly of Applied Mathematics, V. 8, pp. 233-263, November 1955.
4. Dement'eva, K. V. and Aronov, I. Z., "Hydrodynamics and Heat Transfer in Curvilinear Channels of Rectangular Cross Section," Journal of Engineering Physics, V. 34, No. 6, pp. 666-671, 1978.
5. Mayle, R. E., Kopper, F. C., Blair, M. F., and Bailey, D. A., "Effect of Streamline Curvature on Film Cooling," Journal of Engineering for Power, Trans. ASME, V. 99, Series A, No. 1, pp. 77-82, January 1977.
6. Nicolas, J. and LeMeur, A., "Curvature Effects on a Turbine Blade Cooling Film," ASME Paper No. 74-GT-156, 1974.
7. Folayan, C. O. and Whitelaw, J. H., "The Effectiveness of Two-Dimensional Film-Cooling Over Curved Surfaces," ASME Paper No. 76-HT-31, 1976.
8. Lord Rayleigh, "On the Dynamics of Revolving Fluids," Proceedings of The Royal Society of London, Series A, V. 93, pp. 148-154, 1916. Reprints in Scientific Papers, V. 6, pp. 447-453.
9. Taylor, G. I., "Distribution of Velocity and Temperature Between Concentric Rotating Cylinders," Proceedings of the Royal Society of London, Series A, V. 151, pp. 494-512, 1935.
10. Dean, W. R., "Fluid Motion in a Curved Channel," Proceedings of the Royal Society of London, Series A, V. 121, pp. 402-420, 1928.

11. Reid, W. H., "On the Stability of Viscous Flow in a Curved Channel," Proceedings of the Royal Society of London, Series A, V. 244, pp. 186-198, 1958.
12. Schlichting, H., Boundary Layer Theory, 7th Ed., pp. 529-536, McGraw-Hill, 1979.
13. Kelleher, M. D., Flentie, D. L., and McKee, R. J., "An Experimental Study of the Secondary Flow in a Curved Rectangular Channel," Journal of Fluids Engineering, V. 102, pp. 92-96, March 1980.
14. Winoto, S. H., Durao, D. F. G., and Crane, R. I., "Measurement within Gortler Vortices," Journal of Fluids Engineering, V. 101, pp. 517-520, December 1979.
15. Aihara, Y., "Nonlinear Analysis of Gortler Vortices," The Physics of Fluids, V. 19, pp. 1655-1660, November 1976.
16. Kreith, F., "The Influence of Curvature on Heat Transfer to Incompressible Fluids," Trans. ASME, V. 77, pp. 1247-1256, 1955.
17. Aerospace Research Laboratories Reprt ARL 65-68, A Simplified Approach to the Influence of Gortler-Type Vortices on the Heat-Transfer from a Wall, by Leif N. Persen, May 1965.
18. Cheng, K. C., and Akiyama, M., "Laminar Forced Convection Heat Transfer in Curved Rectangular Channels," International Journal of Heat and Mass Transfer, V. 13, pp. 471-490, 1970.
19. Shibani, A. A., and Ozisik, M. N., "A Solution to Heat Transfer in Turbulent Flow Between Parallel Plates," International Journal of Heat and Mass Transfer, V. 20, pp. 65-573, 1977.
20. Mori, Y., Uchida, Y., and Ukon, T., "Forced Convective Heat Transfer in a Curved Channel with a Square Cross Section," International Journal of Heat and Mass Transfer, V. 14, pp. 1787-1805, 1971.
21. Kays, W. M. and Leung, E. Y., "Heat Transfer in Annular Passages - Hydrodynamically Developed Turbulent Flow with Arbitrarily Prescribed Heat Flux," International Journal of Heat and Mass Transfer, V. 6, pp. 507-557, 1963.

22. Brinich, P. F. and Graham, R. W., "Flow and Heat Transfer in a Curved Channel," NASA Technical Note No. TN-D-8464, 1977.
23. McKee, R. J., An Experimental Study of Taylor-Gortler Vortices in a Rectangular Channel, Eng. Thesis, Naval Postgraduate School, Monterey, California, 1973.
24. Durao, M. do Carmo, Investigation of Heat Transfer in Straight and Curved Rectangular Ducts Using Liquid Crystal Thermography, Eng. Thesis, Naval Postgraduate School, Monterey, California, 1977.
25. Ballard, J. C. III, Investigation of Heat Transfer in Straight and Curved Rectangular Ducts, Master's Thesis, Naval Postgraduate School, Monterey, California, 1980.
26. Holihan, R. G., Jr., Investigation of Heat Transfer in Straight and Curved Rectangular Ducts for Laminar and Transition Flows, Master's Thesis, Naval Postgraduate School, Monterey, California, 1981.
27. Daughety, S. F., Experimental Investigation of Turbulent Heat Transfer in Straight and Curved Rectangular Ducts, Master's Thesis, Naval Postgraduate School, Monterey, California, 1983.
28. Wilson, J. L., Experimental Investigation of Turbulent Heat Transfer in Straight and Curved Rectangular Ducts, Master's Thesis, Naval Postgraduate School, Monterey, California, 1984.
29. Gebhart, B., Heat Transfer, 2nd Edition, p. 260, McGraw-Hill, New York, 1971.
30. The American Society of Mechanical Engineers, Supplement to ASME Power Test Codes, Chapter 4, Flow Measurement, p. 25, 1959.
31. Benedict, R. P., Fundamentals of Temperature, Pressure, and Flow Measurements, 2nd Edition, pp. 443-447, John Wiley and Sons, 1969.
32. Shah, R. K. and London, A. L., Laminar Flow Forced Convection in Ducts, Supplement I, pp. 305-312, Academic Press, 1978.
33. Kline, S. J., and McClintock, F. A., "Describing Uncertainties in Single-Sample Experiments," Mechanical Engineering, V. 75, pp. 3-8, January 1953.

END

FILMED

3-86

DTIC